


# Nonreciprocal Thermal Photonics for Energy Conversion and Radiative Heat Transfer

Zhenong Zhang<sup>1</sup> and Linxiao Zhu<sup>1\*</sup>*Department of Mechanical Engineering, The Pennsylvania State University, University Park, Pennsylvania 16802, USA* (Received 31 December 2021; revised 9 May 2022; accepted 21 June 2022; published 4 August 2022)

Controlling emission and absorption, and radiative heat transfer, is important for photonic energy conversion and thermal management. However, the reciprocal emission and absorption and the reciprocal radiative heat transfer in systems that satisfy the Lorentz reciprocity place fundamental constraints on a range of photonic energy-conversion technologies and thermal management. Breaking the Lorentz reciprocity points to important opportunities for realizing photonic energy conversion at the thermodynamic limit and controlling radiative heat transfer at the nanoscale. In this article, we review the development of nonreciprocal thermal photonics for energy conversion and radiative heat transfer. In Sec. II, we discuss Landsberg schemes for reaching the thermodynamic limit in a range of photonic energy-conversion technologies, including harvesting incoming radiation, photovoltaics, harvesting outgoing radiation, thermophotovoltaics, and simultaneously harvesting the sun and outer space. For nonreciprocal photonic energy conversion, it is critical to design nonreciprocal emitters and absorbers. In Secs. III–V, we discuss different approaches to achieving nonreciprocal emission and absorption, including by using magnetic response time-variant systems and optical nonlinearity, respectively. In Sec. III, we discuss achieving nonreciprocal emission and absorption through magnetic response, including by applying an external magnetic field to magneto-optical materials and by using the internal magnetization in magnetic Weyl semimetals. In Sec. IV, we discuss the use of time-variant systems through time modulation for achieving nonreciprocal emission and absorption. We highlight nonreciprocal emission and absorption in a spatiotemporally modulated antenna and photonic refrigeration based on time modulation. In Sec. V, we discuss the use of Kerr nonlinearity for breaking the Lorentz reciprocity and for achieving photonic refrigeration. In Sec. VI, we discuss radiative heat transfer in nonreciprocal materials. We talk about intriguing phenomena of many-body radiative heat transfer in systems that violate the Lorentz reciprocity, including persistent heat current at thermal equilibrium, the photon thermal Hall effect, a nonreciprocal thermal diode, thermal magnetoresistance, and thermal routing. Finally, we provide remarks on challenges and an outlook on future directions in the emerging field of nonreciprocal thermal photonics.

DOI: [10.1103/PhysRevApplied.18.027001](https://doi.org/10.1103/PhysRevApplied.18.027001)

## I. INTRODUCTION

Controlling emission and absorption is important for photonic energy-conversion technologies, such as solar cells, radiative cooling, and thermophotovoltaics, and for communication and thermal management. There have been significant efforts in using photonic structures for controlling thermal emission and absorption [1–3], such as photonic crystals [4–7], metamaterials [8–10], metasurfaces [11,12], and thermal antennas [13,14]. However, emission and absorption processes are typically constrained by a reciprocity relationship. As stated by Kirchhoff's law of thermal radiation [15–18], for an arbitrary emitter, at a given angle and frequency, the spectral angular emissivity equates to its absorptivity at the same angle and frequency.

Such reciprocal emission and absorption place a fundamental constraint on the performance of a broad range of photonic energy-conversion technologies and thermal management.

Breaking the reciprocity relationship between emission and absorption not only provides important opportunities for advanced control of thermal emission and absorption but also provides an avenue to fundamentally improve photonic energy conversion [19–22]. It turns out that Kirchhoff's law of thermal radiation is not required by the second law of thermodynamics, but it is rather due to the Lorentz reciprocity [21,23,24], which is only valid in nonmagnetic, time-invariant, and linear materials. Thus, there are pathways to achieve nonreciprocal emission and absorption by removing any of the three conditions, i.e., through the use of magnetic response, time-variant systems, or optical nonlinearity.

---

\*lqz5242@psu.edu

Radiative heat transfer has drawn great recent interest. Near-field radiative heat transfer between two objects separated by a subwavelength distance can greatly exceed the blackbody radiation limit [25–40] due to the contribution of surface and evanescent modes. Moreover, in the near field, the spectrum of heat transfer can be quasi-monochromatic [41]. Near-field radiative heat transfer is explored in various structures and materials, such as thin films [29,42–45], metamaterials and metasurfaces [46–49], photonic crystals [50,51], two-dimensional materials [38, 52–56], and hyperbolic materials [57,58]. Owing to its super-Planckian and quasi-monochromatic features, near-field radiative heat transfer has shown great potential for applications such as thermophotovoltaics [59–66], electroluminescent cooling [67–71], thermal diodes [72–82], thermal transistors [83–85], thermal switches [40,52,54, 86–88], heat-assisted magnetic recording [89], and lithography [90]. However, in systems made of materials that satisfy the Lorentz reciprocity, radiative heat transfer is reciprocal [91], significantly constraining its functionality. Breaking the Lorentz reciprocity opens up intriguing opportunities for controlling radiative heat transfer at the nanoscale.

Here, we review the development of nonreciprocal photonic energy conversion and radiative heat transfer in nonreciprocal materials. The review includes the following sections. In Sec. II, we discuss the use of nonreciprocal systems for achieving photonic energy conversion at the thermodynamic limit. To enable energy conversion based on nonreciprocal systems, it is critical to develop nonreciprocal emitters and absorbers. In Secs. III–VI, we discuss recent advances on nonreciprocal emission and absorption, as well as radiative heat transfer in materials that break the Lorentz reciprocity. In Sec. III, we discuss using the magnetic response to achieve nonreciprocal emission and absorption. In Sec. IV, we discuss using time-variant systems via time modulation to achieve nonreciprocal emission and absorption. In Sec. V, we discuss using Kerr nonlinearity to achieve nonreciprocal emission and absorption. In Sec. VI, we discuss radiative heat transfer in nonreciprocal materials. Finally, we discuss challenges and provide an outlook on future directions in the emerging research field of nonreciprocal thermal photonics for energy conversion and radiative heat transfer.

## II. NONRECIPROCAL PHOTONIC ENERGY CONVERSION

Achieving electromagnetic nonreciprocity is essential for realizing photonic energy conversion at the thermodynamic limit [19–22]. The sun, at a surface temperature of about 6000 K, is one of the most important energy resources for human beings. Much research is devoted to understanding the efficiency limit for harvesting solar energy [92–96]. For harvesting incoming radiation from a

source, such as the sun, a good reciprocal absorber must emit radiation towards the source, due to the reciprocity between emission and absorption. Such emission of radiation towards the source cannot be reused and represents a fundamental mechanism for energy loss.

### A. Harvesting incoming radiation

A nonreciprocal scheme is considered to harvest incoming radiation at the thermodynamic limit [21]. Radiation from a source at temperature  $T_H$  enters a circulator and is absorbed by body 1 at a temperature of  $T_1 = T_H$ . However, radiation from body 1 is not sent back to the source, but is routed by the circulator towards body 2 at  $T_2$  [Fig. 1(a)]. Likewise, through a circulator, a body absorbs radiation from a previous body and emits radiation towards a later body. The thermal radiation emitted by the final body at temperature  $T_\infty = T_C$  is sent all the way through the circulators back to the source. A Carnot heat engine is assumed to operate between each body and the ambient environment at temperature  $T_C$ . With an infinite number of bodies with  $T_H = T_1 > T_2 > T_3 > \dots > T_\infty = T_C$ , the efficiency for harvesting the incoming radiation approaches the Landsberg limit [96] as  $\eta_{\text{Landsberg}} = 1 - (4/3)(T_C/T_H) + (1/3)(T_C/T_H)^4$ . For harvesting radiation from the sun with  $T_H = 6000$  K and in an ambient environment with  $T_C = 300$  K, the Landsberg limit amounts to 93.3%, which significantly exceeds the limiting efficiency for harvesting incoming radiation using reciprocal systems of 86.8% [20,93–95]. From an entropic point of view, the Landsberg scheme [Fig. 1(a)] avoids additional entropy generated in the bodies beyond the intrinsic entropy generation in the radiative exchange [20,97], thus leading to the thermodynamic limit for harvesting incoming radiation.

Harvesting incoming radiation using nonreciprocal systems is considered using time-asymmetric photovoltaics in a reflection-based setup [19]. A reciprocal solar cell needs to emit luminescence towards the sun. Such luminescence represents a fundamental energy-loss mechanism. Harvesting such luminescence requires the use of a nonreciprocal emitter, which features a large contrast between the emissivity and absorptivity in the same direction. By using a solar cell that behaves as a nonreciprocal emitter, its luminescence can be sent in a direction different from the sun, and therefore, can be reharvested by another solar cell, improving the overall efficiency [19] [Fig. 1(b)]. By using an array of nonreciprocal solar cells, the efficiency can approach the Landsberg limit of 93.3%, which is significantly higher than the efficiency limit for time-symmetric photovoltaics of 86.8% [93–95].

Recently, a simplified scheme for reaching the Landsberg limit was introduced by using a nonreciprocal multi-junction solar cell based on semitransparent nonreciprocal absorbers [Fig. 1(c)] [98]. The nonreciprocal multijunction solar cell consists of multiple layers, where each layer

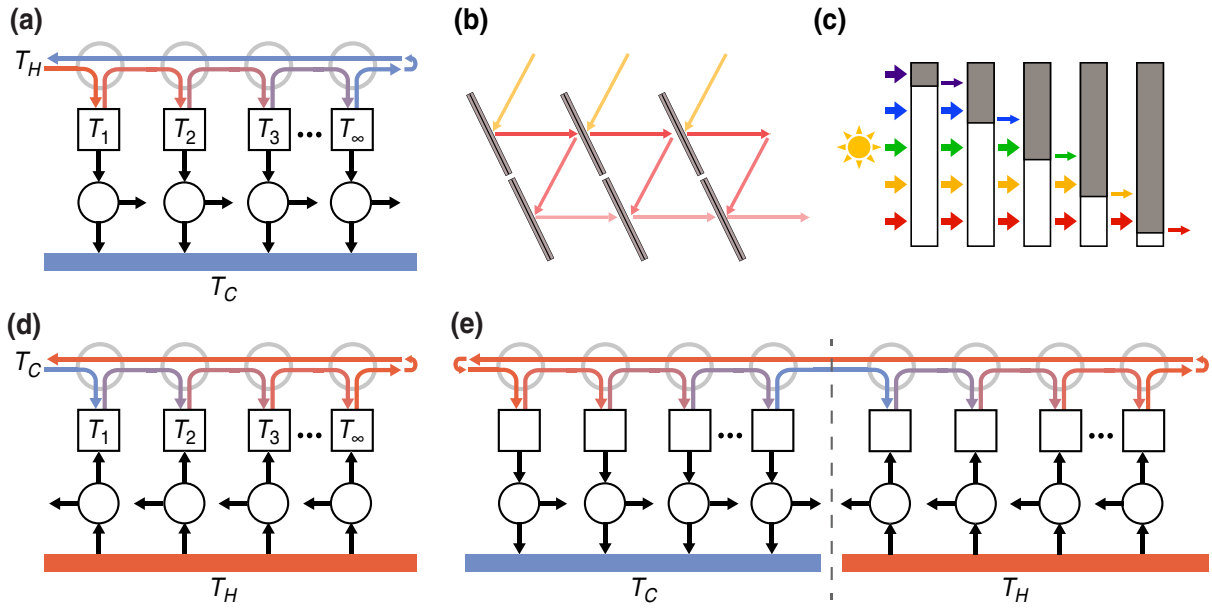


FIG. 1. Landsberg limit for harvesting incoming radiation and outgoing radiation. (a) Scheme for harvesting incoming radiation. Gray circles denote circulators for radiation. (b) Time-asymmetric photovoltaics in a reflection-based setup [19]. (c) Nonreciprocal multijunction solar cell based on semitransparent nonreciprocal absorbers [98]. (d) Scheme for harvesting outgoing thermal radiation [20]. (e) Scheme for thermophotovoltaics [20].

behaves as a semitransparent nonreciprocal absorber [99]. Sunlight from the left irradiates on a high-band-gap solar cell, which is a semitransparent nonreciprocal absorber. At below-band-gap frequencies, light passes through the absorber. At above-band-gap frequencies, the nonreciprocal absorber absorbs light from the left, but emits luminescence towards the right [99]. Similarly, the transmitted light and luminescence can be harvested using a series of semitransparent nonreciprocal absorbers with increasingly lower band gaps. The Landsberg limit can be approached using an infinite number of semitransparent nonreciprocal absorbers.

### B. Harvesting outgoing radiation and thermophotovoltaics

On the other side of the sky, outer space at 3 K is being explored as an emerging renewable resource [20,100]. The earth's atmosphere is highly transparent at wavelengths between 8 and 13  $\mu\text{m}$ , which is known as the atmospheric transparency window. There have been great advances in passive radiative cooling to subambient temperatures, even under direct sunlight, by sending heat through the atmospheric transparency window to cold outer space [101–122]. Also, there has been interest in harvesting the outgoing thermal radiation towards outer space to produce electricity [100,123–126].

The Landsberg scheme is introduced for harvesting outgoing thermal radiation between an ambient

environment at  $T_H$  and a heat sink at  $T_C$ , as illustrated in Fig. 1(d) [20]. Body 1 absorbs radiation from a heat sink at temperature  $T_C$ , but the radiation of body 1 is routed by a circulator towards body 2. Likewise, through a circulator, a body absorbs radiation from a previous body and sends its radiation towards a later body. A final body emits its radiation all the way through the circulators to the heat sink. A Carnot heat engine is assumed to operate between the ambient environment and each body. Using an infinite number of bodies with  $T_C = T_1 < T_2 < T_3 < \dots < T_\infty = T_H$ , the maximum total power generated is  $\sigma((1/3)T_H^4 - (4/3)T_H T_C^3 + T_C^4)$ , where  $\sigma$  is the Stefan-Boltzmann constant. Here, the circulators are assumed to operate over broadband and over the whole  $4\pi$  solid angle. For  $T_H$  at 300 K and  $T_C$  at 3 K, such a Landsberg scheme generates a total power of 153.1  $\text{W}/\text{m}^2$ . Such power output in the Landsberg scheme is significantly higher than the maximum power of 55.0  $\text{W}/\text{m}^2$  generated by using reciprocal systems [20,100,123], highlighting the significant potential of using nonreciprocal systems for harvesting outgoing thermal radiation.

For harvesting incoming radiation and outgoing radiation, a heat engine is operated at the cold side and the hot side, respectively. In thermophotovoltaics, both the hot and cold sides are accessible. It has been pointed out that by connecting the Landsberg scheme for harvesting incoming radiation [Fig. 1(a)], and that for harvesting outgoing radiation [Fig. 1(d)], the Carnot efficiency can be achieved with maximum power output [20] [Fig. 1(e)].

**C. Simultaneously harvesting the sun and outer space**

With both the sun and outer space as resources from the sky, there are emerging interests in simultaneously harvesting the sun and outer space for energy [111,122,127]. Landsberg schemes are introduced for simultaneously harvesting the sun and outer space [22]. First, a Landsberg scheme for harvesting sunlight with combined radiative cooling is considered [Fig. 2(a)] [22]. The cell is thermally insulated from the ambient environment, and its temperature is determined by radiative heat exchange. The system can reach a maximal efficiency of 95.9% with an optimal cell temperature of 185 K, which significantly exceeds the typical Landsberg limit of 93.3%. Here, the efficiency is normalized by the solar irradiance power, and such a convention is used throughout the discussion of simultaneous energy harvesting.

Likewise, a Landsberg scheme for harvesting outgoing radiation combined with solar heating is considered [Fig. 2(b)] [22]. The cell is thermally insulated from the ambient environment, and its temperature is determined by radiative exchange. The system reaches a maximum work of 400.5 W/m<sup>2</sup> and an efficiency of 25.0%, with a cell temperature of 381.5 K.

Then a Landsberg setup combining both incoming and outgoing radiation is considered in Fig. 2(c) [22]. The cell is in good thermal contact with the ambient environment

at 300 K. In such a scheme, the maximum work that can be generated is 1648.2 W/m<sup>2</sup>, corresponding to an efficiency of 102.89%. The maximum work here significantly exceeds what is possible by harvesting the incoming radiation or the outgoing radiation alone.

Alternatively, a Landsberg setup combining both incoming and outgoing radiation is considered in Fig. 2(d) [22], where the cell is thermally isolated from the ambient environment and its temperature is determined by radiative exchange. The system achieves a maximal efficiency of 97.2%, with an optimal cell temperature of 167.6 K. The efficiency in a such scheme is also higher than the typical Landsberg limit of 93.3%. These results highlight the great potential for simultaneously harvesting the sun and outer space for energy.

**III. NONRECIPROCAL EMISSION AND ABSORPTION USING MAGNETIC RESPONSE**

To reach the thermodynamic limit for harvesting incoming radiation, harvesting outgoing radiation, thermophotovoltaics, and simultaneously harvesting the sun and outer space, it is essential to break the Lorentz reciprocity. One approach to break the Lorentz reciprocity is to use materials with an asymmetric permittivity tensor,  $\bar{\epsilon}$ , or permeability tensor,  $\bar{\mu}$ , i.e.,  $\bar{\epsilon} \neq \bar{\epsilon}^T$  or  $\bar{\mu} \neq \bar{\mu}^T$  where  $T$  denotes

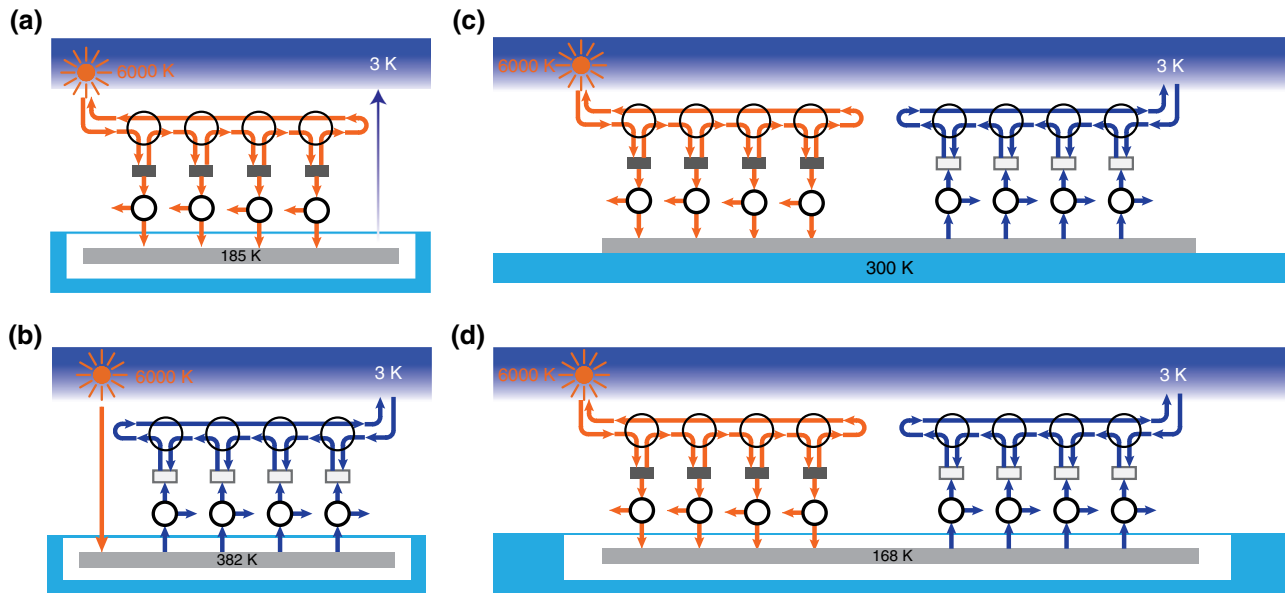


FIG. 2. Landsberg limit for simultaneous energy harvesting. (a) Scheme for Landsberg-limit system for harvesting incoming radiation combined with radiative cooling. Photovoltaic cell is thermally insulated from the ambient environment, and equilibrium temperature is determined by radiative exchange to be 185 K [22]. (b) Scheme for Landsberg-limit system for harvesting outgoing radiation combined with solar heating. Cell is thermally insulated from the ambient environment, and equilibrium temperature is determined by radiative exchange to be 382 K [22]. (c),(d) Schemes of a Landsberg-limit system combining both incoming radiation and outgoing radiation [22]. (c) Case where the cell is in good thermal contact with the ambient environment at 300 K. (d) Case where the cell is thermally insulated from the environment at 300 K, and equilibrium temperature is determined by radiative exchange to be 168 K.

the transpose of a matrix [24,128,129]. For a magneto-optical material in the presence of an external magnetic field, its permittivity is described by an asymmetric tensor. The asymmetric permittivity tensor in magneto-optical materials arises from the cyclotron motion of charge carriers subject to a magnetic field [130]. Breaking the Lorentz reciprocity with magneto-optical materials is used to design optical isolators and circulators, which allows light to transmit in the forward direction but blocks it in the reverse direction. It is noteworthy that nonreciprocal light transmission does not violate the second law of thermodynamics [131]. Alternatively, magnetic materials can break the Lorentz reciprocity due to internal magnetization. One type of candidate material is the recently discovered magnetic Weyl semimetals (WSMs) [132–136], which can break the Lorentz reciprocity and time-reversal symmetry, even in the absence of an external magnetic field, owing to the large anomalous Hall effect associated with enhanced Berry curvature at the Weyl nodes.

### A. Nonreciprocal emission and absorption using external magnetic field

To achieve nonreciprocal photonic energy conversion at the thermodynamic limit, it is essential to completely break Kirchhoff's law of thermal radiation, i.e., to achieve unity difference between emissivity and absorptivity at the same angle and frequency. A principle for completely breaking Kirchhoff's law is introduced for a specular thermal emitter [137]. Figure 3(a) shows an emitter in thermal equilibrium with two blackbodies  $A$  and  $B$ . At thermal equilibrium, the net energy flow in and out of blackbody  $A$  is zero. On one hand, for the radiation of blackbody  $A$  emitted towards the emitter, part of it is absorbed with absorptivity  $\alpha_A$ , and the remaining is reflected towards  $B$  with reflectivity  $r_{A \rightarrow B}$ . On the other hand, the radiation towards  $A$  consists of the radiation of the emitter with emissivity  $e_A$ , and the radiation of blackbody  $B$  reflected by the emitter with reflectivity  $r_{B \rightarrow A}$ . Energy conservation leads to  $e_A - \alpha_A = r_{A \rightarrow B} - r_{B \rightarrow A}$ . Thus, to achieve unity difference between emissivity and absorptivity, the reflectivity needs to be nonreciprocal and there needs to be unity difference between the reflectivities in two directions, i.e.,  $|r_{A \rightarrow B} - r_{B \rightarrow A}| = 1$ . Nonreciprocal reflectivity can be achieved in magneto-optical materials with external magnetic field [138]. Based on coupled-mode theory, completely breaking Kirchhoff's law requires critical coupling of the intrinsic decay rate,  $\gamma_i$ , and external decay rate,  $\gamma_e$ , i.e.,  $\gamma_i \approx \gamma_e$ , and having a nonreciprocity-induced resonant frequency shift,  $\Delta\omega$ , exceeding decay rates, i.e.,  $\Delta\omega \gg \gamma_{i,e}$  [137].

A one-dimensional grating of  $n$ -InAs atop aluminum is analyzed [Fig. 3(b)]. Direct calculation of emissivity using fluctuational electrodynamics revealed near-complete breaking of Kirchhoff's law of thermal radiation,

when there is a 3-T magnetic field applied in the Voigt geometry [Fig. 3(c)]. The grating couples a nonreciprocal guided mode to the far field. At  $\theta = 61.28^\circ$  and TM polarization, there is near-unity difference between the emissivity and absorptivity.

To reduce the magnetic field, an emitter with higher-quality resonance is designed that consists of an InAs film sandwiched by a top low-loss dielectric grating and a bottom aluminum layer [141]. Due to reduced decay rates, a smaller resonance frequency shift can be sufficient to satisfy the requirement  $\Delta\omega \gg \gamma_{i,e}$ . Accordingly, a near-complete violation of Kirchhoff's law is shown at a smaller magnetic field of 0.3 T [141].

### B. Nonreciprocal emission and absorption using magnetic Weyl semimetals

Achieving nonreciprocal emission and absorption using magneto-optical materials requires an external magnetic field. In contrast, magnetic WSMs [132–136] can break the Lorentz reciprocity and time-reversal symmetry in the absence of an external magnetic field, owing to a large anomalous Hall effect associated with enhanced Berry curvature at the Weyl nodes. For type-I WSMs, the vector  $2\mathbf{b}$  separating two Weyl cones in momentum space acts similarly to an internal magnetic field, as illustrated in Figs. 3(d) and 3(g). WSM-based emitters can break Kirchhoff's law of thermal radiation even without a magnetic field [139,140]. A grating of WSM is considered with momentum separation  $2\mathbf{b}$  in the Voigt geometry [Fig. 3(e)] [139]. Direct calculation shows that in TM polarization, Kirchhoff's law of thermal radiation can be strongly broken without a magnetic field [Fig. 3(f)]. In another study, a dielectric grating on top of WSM is considered [Fig. 3(h)] [140]. The absorptivities in two opposite directions show a strong contrast, as shown by solid lines in Fig. 3(i). As  $e(\theta) = \alpha(-\theta)$  for a specular emitter [137], the strong contrast between absorptivities in two opposite directions indicates a strong violation of Kirchhoff's law of thermal radiation. Also, the nonreciprocal emission and absorption is robust after accounting for Fermi-arc states [Fig. 3(j)] [140]. In these WSM-based emitters, the nonreciprocal emission and absorption are mediated by nonreciprocal a surface-plasmon polariton, which is coupled to free space through a WSM grating [139] or a low-loss dielectric grating atop a WSM layer [140]. Due to the linear dispersion near Weyl nodes, the emissivity and absorptivity of WSM-based structures have a strong dependence on temperature [139,140]. Magnetic Weyl semimetals have the potential to be used to achieve nonreciprocal emission and absorption without a magnetic field.

There is significant interest in nonreciprocal control of emission and absorption. Nonreciprocal emission and absorption are theoretically studied in different photonic structures, including gratings [137,139–147], photonic



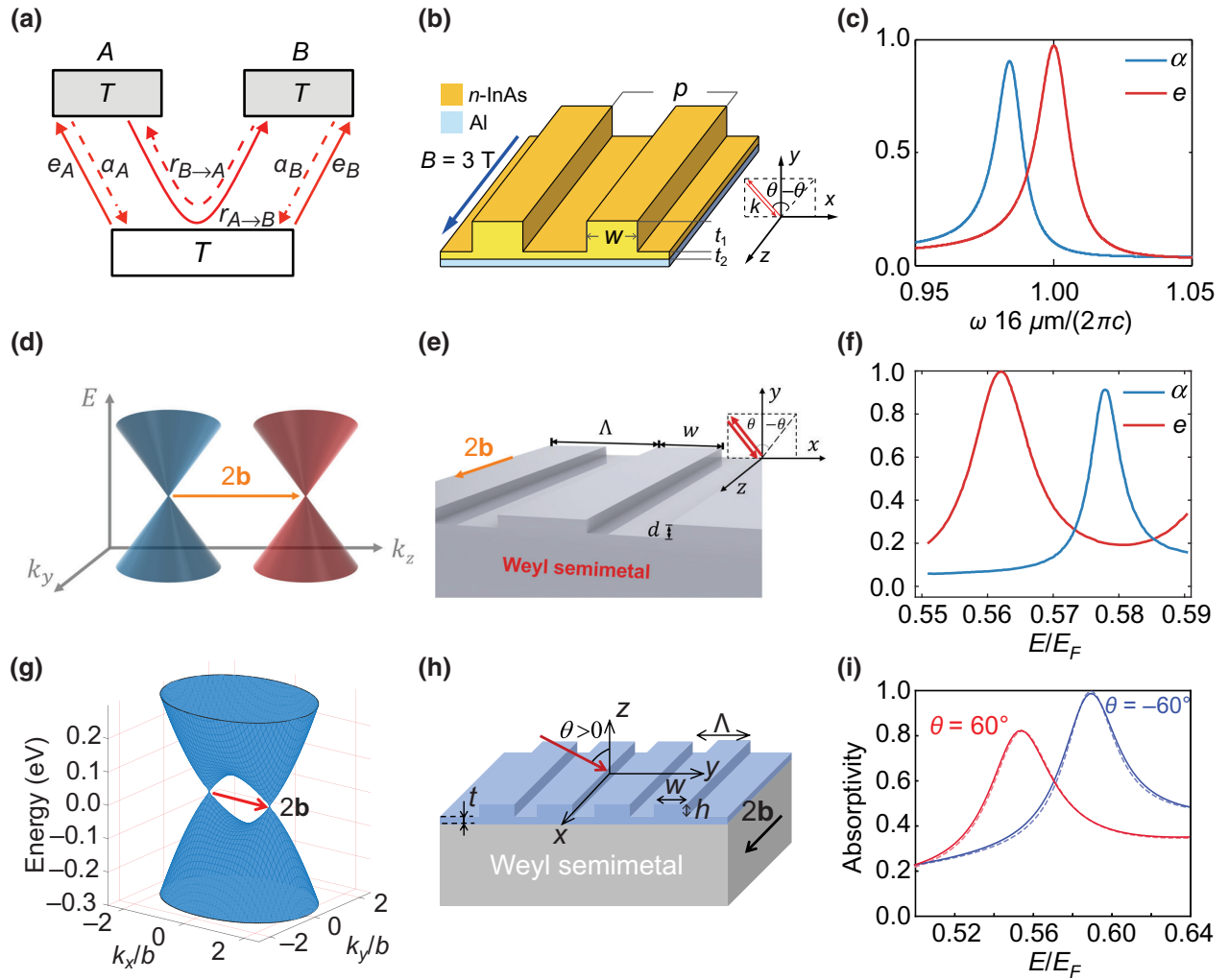


FIG. 3. Nonreciprocal emission and absorption based on magnetic response. (a) Energy balance between a thermal emitter and two blackbodies in thermal equilibrium [137]. (b) Grating of  $n$ -InAs atop aluminum in the presence of a 3-T magnetic field in the Voigt geometry [137]. (c) Absorptivity,  $\alpha$ , and emissivity,  $e$ , spectra of the structure in (b) for TM polarization at  $\theta = 61.28^\circ$  [137]. (d) Electronic band structure of a magnetic Weyl semimetal with two Weyl nodes. Weyl nodes have opposite chirality with  $2\mathbf{b}$  separation in the momentum space [139]. (e) Grating of magnetic Weyl semimetal with its electronic band structure shown in (d) [139]. (f) Absorptivity and emissivity spectra of the structure in (e) for TM polarization at  $\theta = 80^\circ$  [139]. (g) Electronic band structure of a magnetic Weyl semimetal [140]. (h) Dielectric grating on top of magnetic Weyl semimetal with its electronic band structure shown in (g) [140]. (i) Absorptivity spectra of the structure in (h) at  $\theta = 60^\circ$  and  $-60^\circ$ . Solid lines and dashed lines denote results without and with consideration of the Fermi arc states, respectively [140].

crystals [148], thin films [149,150], and substrates [151]. Among them, thin films [149,150] and substrates [151] can simplify the experimental investigation of nonreciprocal emission and absorption owing to the ease of fabrication. Moreover, although most studies focus on opaque emitters, nonreciprocal emission and absorption are also studied in semitransparent structures [99,152]. Also, a diffractive nonreciprocal emitter is used to further break the symmetry between  $e(\theta)$  and  $\alpha(-\theta)$  [143], which can provide more flexibility in the design of nonreciprocal emitters and absorbers. Finally, we note that, for an arbitrary thermal

emitter, universal modal radiation laws are introduced that work regardless of reciprocity [153]. In a mode-converter input and output mode sets, the absorptivity of any input mode equals the emissivity into the corresponding output mode, and the sum of absorptivities of any complete set of input modes is equal to the sum of emissivities of any complete set of output modes, which are valid, even for nonreciprocal emitters [153]. Such universal radiation laws place constraints on the emission and absorption processes in nonreciprocal emitters, and thus, can be useful in designing nonreciprocal emitters.

#### IV. NONRECIPROCAL EMISSION AND ABSORPTION IN TIME-VARIANT SYSTEMS

Time modulation provides a magnet-less alternative to breaking the Lorentz reciprocity. Conventional nonreciprocal optical components based on magneto-optical materials, such as isolators and circulators, are bulky and incompatible with complimentary metal oxide semiconductor (CMOS) technology. Advances in breaking reciprocity using time modulation lead to one-way transmission of light without using a magnetic field [154–158]. Recently, time modulation was used to achieve nonreciprocal emission and absorption [159], photonic refrigeration [160], and a thermal radiation pump [161–163].

##### A. Nonreciprocal emission and absorption using spatiotemporal modulation

Nonreciprocal emission and absorption based on time-variant systems are experimentally demonstrated at radio frequencies [159]. A periodically loaded open waveguide is designed, as shown in Figs. 4(a) and 4(b). Spatial and temporal modulation of capacitors creates intraband transitions, leading to nonreciprocal radiation. When there is no modulation, at the same frequency, the transmitting and receiving radiation patterns are measured to be same. On the other hand, when there is strong modulation, the contrast between the transmitting and receiving radiation patterns can reach 15 dB ( $\sim 30$ -fold) at the same frequency and angle [Figs. 4(c)–4(f)]. Such an approach has potential for radio-frequency communication and could be useful for energy harvesting and thermal management if translated to infrared frequencies. It is noteworthy that state-of-the-art graphene modulators have an intrinsic modulation frequency of 150 GHz [164], which is about 2 orders of magnitude smaller than the peak frequency for thermal radiation at 300 K. Thus, breaking the reciprocity by using time modulation can be relevant for achieving nonreciprocal thermal emission.

##### B. Photonic refrigeration using time modulation

It has been discovered that time modulation can be used for photonic refrigeration [160]. A cavity supports two modes, 1 and 2, at resonant frequencies  $\omega_1$  and  $\omega_2$ , respectively [Fig. 5(a)], with  $\omega_1 < \omega_2$ . In a temporal coupled-mode model, mode 1 has a finite internal decay rate,  $\gamma_1^i$ , coupled to an internal heat bath at temperature  $T_c$  and zero external decay rate,  $\gamma_1^e = 0$ . On the other hand, mode 2 has zero internal decay rate,  $\gamma_2^i = 0$ , and a finite external decay rate,  $\gamma_2^e$ , coupling to an external heat bath at temperature  $T_h$ . In the absence of modulation, modes 1 and 2 are uncoupled; thus, there is no electromagnetic energy transfer between the refrigerator and its surroundings. Modulating the cavity at a frequency of  $\Omega = \omega_2 - \omega_1$  couples the two modes, while conserving the total photon

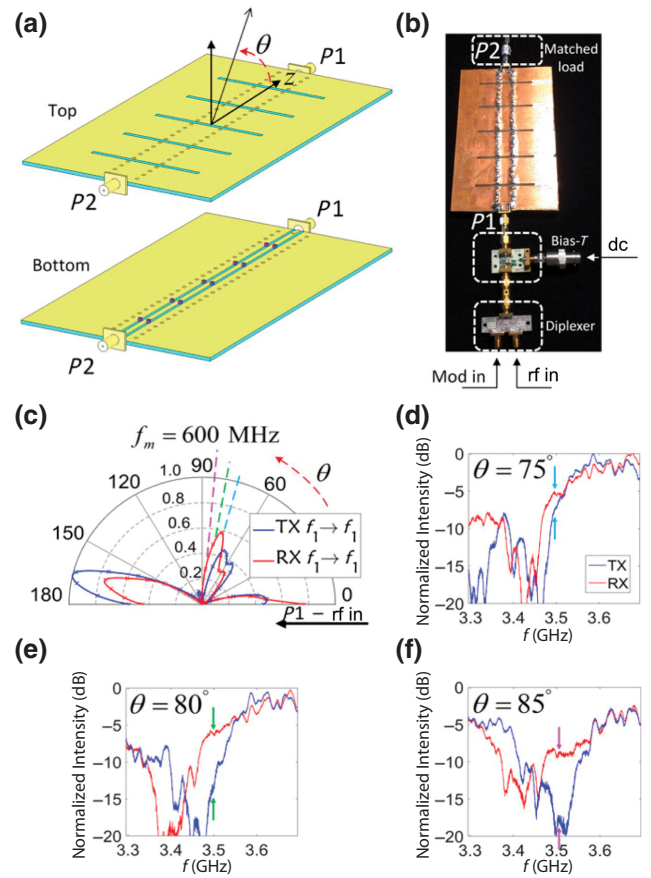


FIG. 4. Nonreciprocal antenna based on spatiotemporal modulation. (a),(b) Schematic and photograph of a nonreciprocal antenna, respectively [159]. (c) Nonreciprocal radiation at the fundamental frequency with a modulation frequency of 600 MHz. TX and RX denote transmitting radiation and receiving radiation, respectively [159]. Measured radiation-intensity spectra, normalized by the maximum value in (c), at angles of (d)  $\theta = 75^\circ$ , (e)  $80^\circ$ , and (f)  $85^\circ$  [159].

number in the two modes. A coupled-mode-theory analysis reveals a net cooling power, when  $(\omega_2/\omega_1) \geq (T_h/T_c)$ , after accounting for the work input of time modulation [Fig. 5(b)]. The COP is bounded by the Carnot bound, which is approached when the ratio between the frequencies of the two modes matches the ratio between the two temperatures, i.e.,  $(\omega_2/\omega_1) = (T_h/T_c)$  [Fig. 5(c)].

A physical structure for the refrigerator consists of a cavity with two defects, 1 and 2, located in a distributed Bragg reflector [Fig. 5(d)]. The permittivity for defect 2 and the permittivity for the region between these two defects are temporally modulated at the same frequency,  $\Omega$ , and with the same modulation amplitude,  $\delta$ . A rigorous coupled-wave analysis is performed, at a modulation frequency of 1 THz and modulation amplitude of permittivity as 0.5. The photon-transmission functions,  $\Phi$ , in the forward and backward directions are equal in the absence of modulation [Fig. 5(e)]. In contrast, in the presence of

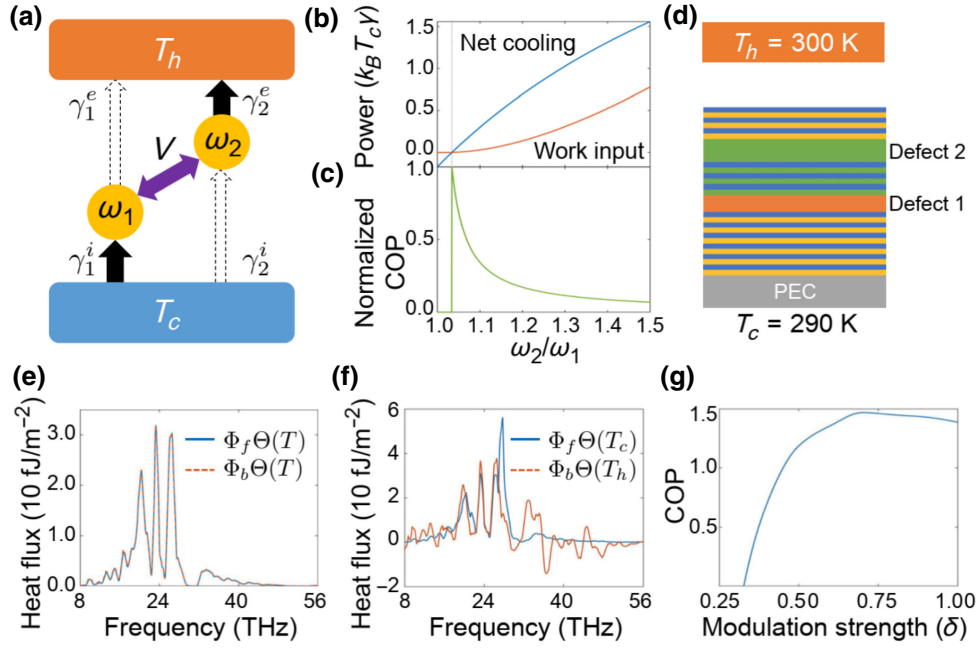


FIG. 5. Photonic refrigeration based on time modulation. (a) Coupled-mode scheme of a photonic refrigerator operating between a cold side,  $T_c$ , and a hot side,  $T_h$ , by coupling two modes at  $\omega_{1,2}$  using time modulation (purple arrow) [160]. (b) Net cooling power and work input evaluated using a coupled-mode model normalized to  $k_B T_c \gamma$  versus the ratio of the frequencies of the two modes for  $T_h = 300$  K and  $T_c = 290$  K,  $V = 2\gamma$ , and  $\gamma = \gamma_1^i = \gamma_2^e$  [160]. (c) Coefficient of performance (COP) normalized to the Carnot bound [160]. (d) Physical structure of a photonic refrigerator [160]. Heat-flux spectrum in forward and reverse directions in the structure of (d) for (e) the unmodulated case at  $T_h = T_c = 300$  K and (f) the modulated case at permittivity modulation strength  $\delta = 0.5$ ,  $T_h = 300$  K, and  $T_c = 290$  K [160]. (g) COP as a function of modulation strength [160].

time modulation, the photon-transmission functions in the two opposite directions become unequal, highlighting non-reciprocal energy transfer [Fig. 5(f)]. It leads to a net cooling power of  $282.2 \text{ mW/m}^2$  and COP of 1.188. The COP can exceed 1.4 by optimizing the modulation strength [Fig. 5(g)]. Photonic refrigeration via time modulation has the potential advantage of being much more efficient than laser cooling [165–167], without a stringent requirement on the quantum efficiency in electroluminescent cooling [67,68,70,168].

## V. NONRECIPROCAL EMISSION AND ABSORPTION USING OPTICAL NONLINEARITY

The Lorentz reciprocity can be broken in nonlinear materials, where the polarization has a nonlinear dependence on the electric field. Optical nonlinearity is used to achieve optical isolation [169–171], although a dynamic reciprocity exists for small-amplitude signal excitations from two opposite directions in the presence of a large driving signal [172].

Kerr  $\chi^{(3)}$  nonlinearity is used for controlling thermal radiation [173,174]. A three-resonator system is considered [Fig. 6(b)] [173]. Two resonators, with resonant frequencies  $\omega_1$  and  $\omega_3$ , are coupled to two thermal reservoirs. A third resonator with resonant frequency

$\omega_2 = (\omega_3 - \omega_1)/2$  is excited by laser irradiance and placed in a nonlinear material with  $\chi^{(3)}$  nonlinearity. Through a four-wave mixing process, photons in resonators 1 and 3 are coupled through the interaction with excited photons in resonator 2. In such a four-wave mixing process, the total photon number is conserved, and the coupling between resonance mode 1 and resonance mode 3 is nonreciprocal. The physical construction of such a scheme involves an ITO absorber (resonator 3) and a SiC emitter (resonator 1), with a nonlinear  $\chi^{(3)}$  spacer in between [Fig. 6(a)]. The two substrates support surface polaritons at disparate frequencies. To enhance the nonlinear response, a strongly localized plasmonic resonance is created by embedding graphene nanodisks in the nonlinear material. Calculations based on coupled-mode theory show heat is extracted from the SiC emitter [Fig. 6(c)], even when the two substrates are at the same temperature. The heat extracted from the SiC emitter increases as the laser intensity increases and can greatly exceed the radiative heat transfer driven by a temperature difference between 300 and 0 K. It is noted that the lossy plasmonic resonances lead to a high power requirement of  $10^{12} \text{ W/m}^2$ .

Near-field refrigeration is further analyzed in a system with low-loss dielectric resonances [Fig. 6(d)] [174]. The system includes a  $\text{SiO}_2$  emitter and an absorber consisting of an AZO, a CG layer, and dielectric grating. With



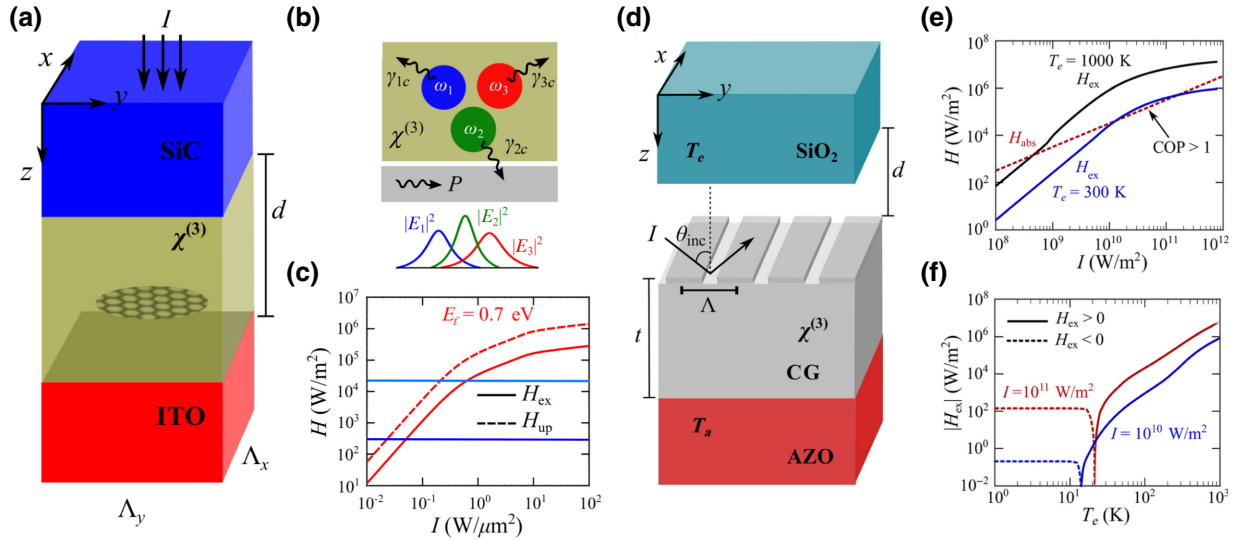


FIG. 6. Heat extraction based on Kerr nonlinearity. (a) Geometry of a system consisting of an indium tin oxide (ITO) absorber covered by a 60-nm-thick nonlinear chalcogenide (CG) film and a SiC emitter. Square lattice of graphene nanodisks with 20-nm radius and 60-nm periodicity is embedded in the nonlinear medium and is 10 nm away from the ITO layer. Pump light is vertically incident on the structure [173]. (b) Schematic of three resonators at equal temperature supporting modes at  $\omega_j$ , each with decay rate  $\gamma_j$ , with  $j = \{1, 2, 3\}$ . Modes 1 and 3 are coupled to each other through a four-wave mixing process involving a Kerr  $\chi^{(3)}$  medium excited by incident light of power  $P$  from a waveguide coupled to mode 2 [173]. (c) Heat-extraction power,  $H_{\text{ex}}$ , from the emitter and upconverted power,  $H_{\text{up}}$ , as compared with temperature-driven radiative heat transfer between two vacuum-separated SiC plates held at 300 K (light blue) and 1 K (dark blue) temperature differences. Graphene has a Fermi energy of 0.7 eV [173]. (d) Geometry of a system consisting of an absorber combining aluminum zinc oxide (AZO) and a 100-nm-thick CG layer with dielectric grating and a SiO<sub>2</sub> emitter, separated by a vacuum gap with size  $d = 30$  nm [174]. (e) Heat-extraction power from the SiO<sub>2</sub> emitter versus intensity, for the SiO<sub>2</sub> emitter at 1000 and 300 K, respectively. Power absorbed in the absorber is also shown [174]. (f) Heat-extraction power of the SiO<sub>2</sub> emitter versus emitter temperature at two intensity levels  $I = 10^{10}$  and  $10^{11}$  W/m<sup>2</sup>. Absorber is at 300 K [174].

the absorber at 300 K and the emitter at 1000 K, a large heat-extraction rate of  $10^5$  W/m<sup>2</sup> can be reached at a moderate drive intensity on the order of  $10^9$  W/m<sup>2</sup> [Fig. 6(e)], which is over 3 orders of magnitude smaller than that of the design using lossy plasmonic resonances [Fig. 6(c)]. The coefficient of performance can exceed unity. Moreover, refrigeration is predicted to function down to the order of tens of kelvin, with the absorber fixed at 300 K [Fig. 6(f)]. The study shows the significant potential of refrigeration using Kerr nonlinearity. The analysis of radiative heat transfer involving a nonlinear medium uses temporal coupled-mode theory [173,174]. Rigorous calculations of radiative heat transfer involving a nonlinear medium using fluctuational electrodynamics [175] would be useful, but challenging, for confirming the results.

## VI. RADIATIVE HEAT TRANSFER IN NONRECIPROCAL MATERIALS

Breaking Lorentz reciprocity using magnetic response time-variant systems and optical nonlinearity provides approaches for achieving nonreciprocal emission and absorption, which is required for developing photonic energy conversion and thermal management based on nonreciprocal devices. On the other hand, there is great interest

in using nonreciprocal materials to control radiative heat transfer, leading to a range of intriguing phenomena.

### A. Persistent heat current at thermal equilibrium

Heat transfer is usually driven by temperature gradient. However, in charge and mass phenomena, such as superconductivity and superfluidity, there can exist a current that persists without any external bias. Recently, it has been pointed out that a persistent heat current can exist at thermal equilibrium in many-body systems where the Lorentz reciprocity is broken [91]. For systems consisting of two bodies, the second law of thermodynamics requires that the net radiative heat-transfer power between the two bodies is zero at thermal equilibrium. Thus, the minimal system to support persistent heat current involves three bodies. A three-body system is considered that consists of three  $n$ -InSb spheres forming an equilateral triangle with an external magnetic field applied orthogonal to the plane of the spheres [Fig. 7(a)]. A scattering approach [176] is used to calculate radiative heat transfer between each pair of bodies, while considering multiple scattering and nonreciprocity. With a 3- $T$  external magnetic field and at thermal equilibrium, the Poynting flux, driven by thermal noise sources in the spheres and the environment,

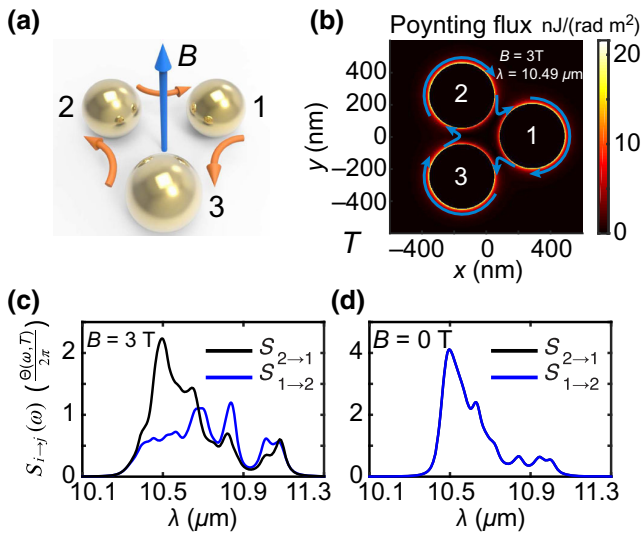


FIG. 7. Persistent heat current at thermal equilibrium. (a) Schematic of a system at thermal equilibrium consisting of three  $n$ -InSb spheres with 200-nm radius arranged in an equilateral triangle. Center-to-center distance between two spheres is 500 nm. External magnetic field is applied orthogonal to the plane of spheres [91]. (b) Poynting flux profile in the center plane when there is a 3-T external magnetic field and when the spheres and environment are all at 300 K [91]. (c),(d) Heat-transfer spectra of  $S_{2 \rightarrow 1}$  and  $S_{1 \rightarrow 2}$ . Here,  $S_{i \rightarrow j}$  denotes the power absorbed by body  $j$  due to thermal noise sources in body  $i$  [91]. (c) Nonreciprocal case with  $B = 3$  T. (d) Reciprocal case with  $B = 0$  T.

shows a persistent heat current [Fig. 7(b)]. At  $10.49 \mu\text{m}$ , there is a global energy flux surrounding the spheres in the clockwise direction. With the external magnetic field, the heat-transfer spectra between two bodies in two opposite directions show strong contrast [Fig. 7(c)]. Even after spectral integration, the contrast of heat transfer in the two opposite directions persists. In contrast, when there is no external magnetic field, the heat-transfer spectra in the two opposite directions are identical to each other, as shown in Fig. 7(d). Such a persistent heat current arises from the fact that, when Lorentz reciprocity is obeyed, the system supports degenerate collective counter-rotating resonance modes. When the Lorentz reciprocity is broken, the degeneracy is lifted, leading to a persistent directional heat current. It should be noted that, for the persistent heat current to exist, the Lorentz reciprocity must be broken [91,177].

### B. Photon thermal Hall effect and anomalous photon thermal Hall effect

A photon thermal Hall effect is predicted in a system consisting of four  $n$ -InSb nanospheres arranged in a square [178]. In analogy to the electronic Hall effect, in the thermal Hall effect, a transversal temperature gradient arises in response to a longitudinal temperature bias

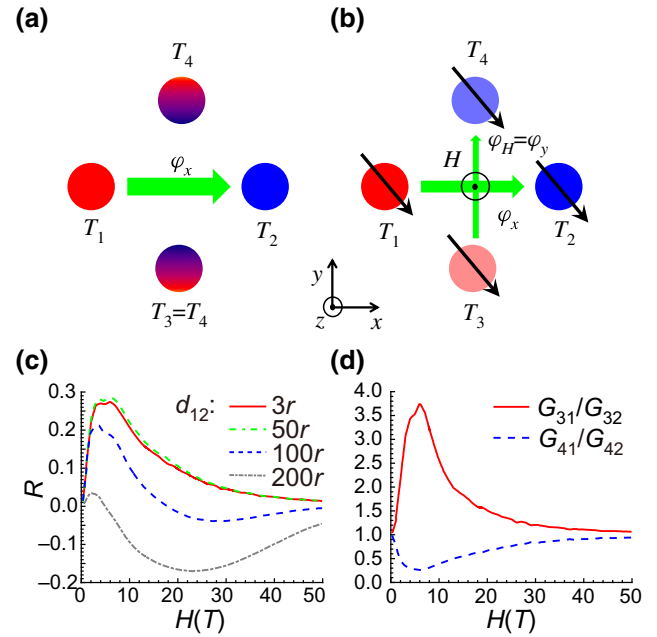


FIG. 8. Photon thermal Hall effect. (a),(b) Schematic of a system consisting of four  $n$ -InSb nanospheres arranged in a square. Two spheres, 1 and 2, along a diagonal line are connected with a hot thermal reservoir and a cold thermal reservoir, respectively [178]. (a) In the absence of external magnetic field, there is no transversal temperature difference between spheres 3 and 4. (b) In the presence of a magnetic field applied orthogonal to the plane of the spheres, a transversal temperature difference develops. (c) Relative Hall temperature difference,  $R$ , versus magnetic field, with particles of radius  $r = 100$  nm at an equilibrium temperature of 300 K. Edge-to-edge separation distance,  $d_{12}$ , between spheres 1 and 2 is  $3r$ ,  $50r$ ,  $100r$ , and  $200r$  [178]. (d) Asymmetry of conductances when  $d_{12} = 3r$  [178].

and an out-of-plane magnetic field. As shown in Fig. 8(a), spheres 1 and 2 along a diagonal line are connected with a high-temperature reservoir and low-temperature reservoir, respectively, while the temperatures of the two other spheres are determined by radiative heat exchange. In the absence of an external magnetic field, there is no transversal temperature difference between spheres 3 and 4 due to mirror symmetry. However, in the presence of a vertical magnetic field, a transversal temperature difference between spheres 3 and 4 develops [Fig. 8(b)]. The photon thermal Hall effect is evaluated using the relative Hall temperature difference,  $R = (T_3 - T_4)/(T_1 - T_2)$ . The relative Hall temperature difference shows a nonmonotonic dependence on the magnetic field and can reach 28% when  $H = 3$  T [Fig. 8(c)]. The existence of the transversal temperature gradient can be understood by the fact that the radiative conductance from sphere 3 to 1 dominates that from sphere 3 to 2, while simultaneously the radiative conductance from sphere 4 to 2 dominates that from sphere 4 to 1 [Fig. 8(d)]. The photon thermal Hall effect can potentially be used for thermal magnetometry.

Moreover, an anomalous photon thermal Hall effect is introduced in a system consisting of four magnetic Weyl semimetal nanoparticles [179], where a transversal temperature gradient arises upon a longitudinal temperature bias, even in the absence of any external magnetic field.

For the four-particle system with  $C4$  symmetry considered in the photon thermal Hall effect [178] and the anomalous photon thermal Hall effect [179], the existence of the thermal Hall effect requires nonreciprocal radiative heat transfer [177,179]. On the other hand, the photon thermal Hall effect does not necessarily require nonreciprocal radiative heat transfer and can exist in systems with broken mirror symmetry, such as through uniaxial birefringence [177].

### C. Nonreciprocal thermal diode

A thermal diode allows heat to flow in a forward temperature bias, but blocks heat flow in the reversed temperature bias. Radiative thermal diodes are studied theoretically [72–74,77–82] and experimentally [75,76]. Thermal diodes in two-body systems require temperature-dependent optical properties for the materials and are explored in SiC [72,74],  $\text{VO}_2$  due to the metal-insulator transition [73,75–78], semiconductors [80–82], and superconductors [79]. Recently, the thermal diode has been extended to nonreciprocal many-body systems [180–182]. Such nonreciprocal thermal diodes rely on nonreciprocal radiative heat transfer between two bodies in the presence of other bodies and do not require temperature-dependent optical properties.

A nonreciprocal thermal diode driven by a nonreciprocal surface-plasmon polaritons (SPPs) is designed [180]. The system consists of two InSb magneto-optical nanoparticles above an InSb substrate [Fig. 9(a)]. The two nanoparticles are at temperatures  $T_1$  and  $T_2$ , and the substrate is at temperature  $T_b$ . In the forward case, particle 1 is heated to a temperature,  $T_p$ , higher than its environment, with  $T_1 = T_p > T_2 = T_b$ . In the backward case, particle 2 is heated with  $T_2 = T_p > T_1 = T_b$ . The net power received by the colder particle in the forward and backward cases is  $\Phi_f$  and  $\Phi_b$ , respectively. In such a three-body system with the same temperature between the substrate and the colder particle, the contrast between  $\Phi_f$  and  $\Phi_b$  directly requires nonreciprocal radiative heat transfer between the two particles. A thermal rectification coefficient is further defined as  $\eta = |\Phi_f - \Phi_b| / \max(\Phi_f, \Phi_b)$ . Under an external magnetic field, the InSb substrate supports a nonreciprocal surface-plasmon polariton, driving nonreciprocal radiative heat transfer between the two particles. A high rectification coefficient of about 0.9 is predicted at a magnetic field of 1 T and an interparticle distance of 1  $\mu\text{m}$  [Fig. 9(b)].

In contrast with building a nonreciprocal thermal diode with a magnetic field [180], a magnet-less nonreciprocal

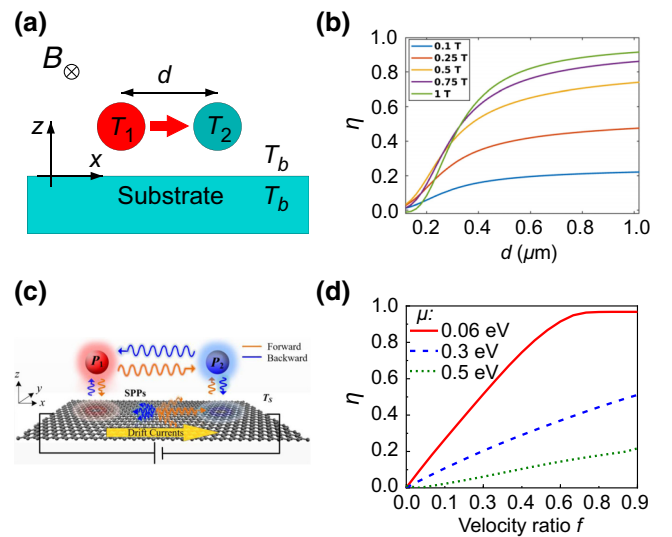


FIG. 9. Nonreciprocal thermal diodes. (a) Schematic of two magneto-optical InSb nanoparticles placed over an InSb substrate. Magnetic field is along the  $y$  axis. Two particles have temperatures  $T_1$  and  $T_2$ , and the substrate has temperature  $T_b$ . Forward case is at  $T_1 = T_p > T_2 = T_b$ , and the backward case is at  $T_2 = T_p > T_1 = T_b$  [180]. (b) Rectification coefficient,  $\eta$ , for thermal diode in (a) as a function of interparticle distance, at varying magnetic fields. Particles have radii of 5 nm and height  $z = 100$  nm [180]. (c) Schematic of two SiC nanoparticles placed over graphene, with drifting electrons along the  $x$  axis [181]. (d) Rectification coefficient for thermal diode in (c) as a function of velocity ratio,  $f$ , at varying chemical potentials of graphene. Particles have radii of 5 nm, interparticle distance of 100 nm, and height  $z = 25$  nm [181].

thermal diode is studied where the reciprocity is broken by a drift current [181]. The system consists of two SiC nanoparticles above a graphene layer [Fig. 9(c)]. By creating drifting electrons with drifting velocity along the  $x$  axis,  $v_d = v_0 f$ , in response to an in-plane electric field on graphene, the graphene conductivity can be written as  $\sigma^d(\omega, k_x) = (\omega / (\omega - k_x v_d)) \sigma(\omega - k_x v_d)$ . Here,  $v_0 = 10^8$  cm/s is the Fermi velocity of graphene,  $f$  is the velocity ratio,  $k_x$  is the wavevector component of the  $x$  axis, and  $\sigma(\omega)$  is the graphene conductivity in the absence of a drift current. By reversing the propagating direction of the surface-plasmon polariton in graphene via reversing  $k_x$ , it can be observed that the conductivity is changed, i.e.,  $\sigma^d(\omega, k_x) \neq \sigma^d(\omega, -k_x)$ . Such a nonreciprocal surface-plasmon polariton drives nonreciprocal radiative heat transfer between the two particles. A rectification coefficient as high as about 0.97 is predicted at 0.06-eV chemical potential for graphene, and a velocity ratio of  $f = 0.85$ , as shown in Fig. 9(d). The rectification coefficient can be further enhanced in a nonreciprocal thermal diode driven by a nonreciprocal hyperbolic surface-plasmon polariton supported in a drift-biased graphene grating [182].

### D. Thermal magnetoresistance and thermal routing

In the phenomena of persistent heat current, photon thermal Hall effect, and nonreciprocal thermal diodes discussed above, nonreciprocal radiative heat transfer is critical. It should be noted that the radiative heat transfer in many-body systems consisting of materials that violate Lorentz reciprocity is not necessarily nonreciprocal. In the following, we discuss thermal magnetoresistance and thermal routing based on nonreciprocal materials, where nonreciprocity in radiative heat transfer is either absent or weak. These effects involving radiative heat transfer in nonreciprocal materials provide intriguing ways for controlling heat flow.

In analogy to electronic giant magnetoresistance, a giant thermal magnetoresistance is predicted in a linear chain of magneto-optical nanoparticles [183], as shown in Fig. 10(a). By applying a magnetic field orthogonal to the chain, the thermal resistance between two particles can increase by over 2 times [Fig. 10(b)], which is

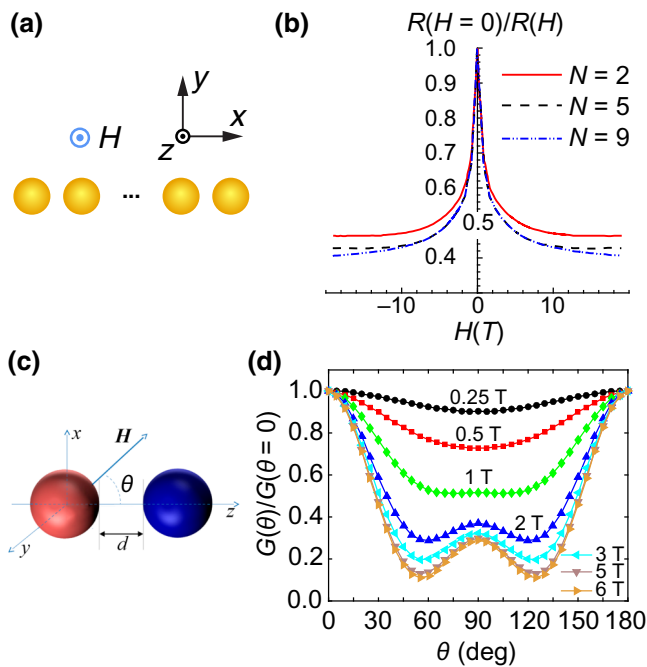


FIG. 10. Giant thermal magnetoresistance and anisotropic thermal magnetoresistance. (a) Schematic of a linear chain of  $N$  identical InSb nanoparticles at 300 K, with an external magnetic field orthogonal to the chain. Radius of each nanoparticle is 100 nm, and the edge-to-edge separation distance between two adjacent particles is 200 nm. (b) Thermal magnetoresistance as a function of the strength of the external magnetic field, for the linear chain in (a) [183]. (c) Schematic of two InSb spheres at 300 K, with magnetic field strength,  $H$ , forming an angle,  $\theta$ , with respect to the vector connecting the centers of spheres [184]. (d) Thermal conductance between the two spheres in (c) as a function of the orientation angle of the magnetic field, for different values of magnetic field [184].

analogous to the magnitude of strong contrast in electronic giant magnetoresistance. Moreover, an anisotropic thermal magnetoresistance is studied [184] in a system consisting of two InSb spheres in the presence of an external magnetic field [Fig. 10(c)]. The radiative thermal conductance is maximized when the magnetic field is aligned with the direction of the two spheres, and the thermal conductance becomes much smaller when the magnetic field is orthogonal to the vector connecting the two spheres [Fig. 10(d)]. The giant thermal magnetoresistance effect and anisotropic thermal magnetoresistance effect could be useful for controlling radiative heat flow using a magnetic field and thermal magnetometry.

A thermal router is designed to control the direction of heat flux by using magnetic Weyl semimetals [185]. It consists of three same-sized nanospheres made of magnetic Weyl semimetals. The centers of the spheres form an isosceles triangle [Fig. 11(a)]. Sphere 1 at the apex has a separation vector connecting the two Weyl nodes of  $2\mathbf{b}_1$ , which can be controlled along the  $z$  direction by using electric, magnetic, or optical fields. The other two spheres, 2 and 3, have fixed separation vectors of Weyl nodes along the  $z$  direction of  $2\mathbf{b}_2 = 1.0 \text{ nm}^{-1}$  and  $2\mathbf{b}_3 = -1.0 \text{ nm}^{-1}$ , respectively. When sphere 1 has separation vector  $2\mathbf{b}_1$  up, the radiative heat transfer between 1 and 3 greatly exceeds that between 1 and 2, routing heat towards sphere 3 [Fig. 11(b)]. In contrast, when the separation vector for sphere 1 is down, heat is routed primarily towards sphere 2. Such a thermal routing effect can be understood by considering thermal emission from a single sphere with separation vector  $2\mathbf{b}$  [Fig. 11(c)]. With a nonzero  $2\mathbf{b}$ , a sphere hosts three nondegenerate dipole modes. The resonant frequency of the mode with zero angular momentum along the  $z$  direction is independent of  $2\mathbf{b}$ , while the resonant frequencies of the two other counter-rotating modes depend on  $2\mathbf{b}$  [Fig. 11(d)]. Between two spheres, with their momentum separation vectors aligned in the vertical direction and antiparallel to each other, resonant-frequency matching and quasi-phase matching are satisfied, leading to strong radiative heat transfer. On the other hand, when the momentum separation vectors of the two spheres are parallel to each other, quasi-phase matching is not achieved for modes with the same resonant frequency, suppressing radiative heat transfer. A thermal router based on magnetic Weyl semimetals could be potentially useful for guiding radiative heat flow by controlling the momentum separation of Weyl nodes in magnetic Weyl semimetals.

Finally, we provide remarks on the reciprocity or nonreciprocity for many-body radiative heat transfer. The radiative heat transfer in many-body systems consisting of materials that break the Lorentz reciprocity is not necessarily nonreciprocal. An approach using the symmetry of a magnetic group and the second law of thermodynamics is introduced to determine the reciprocity or nonreciprocity



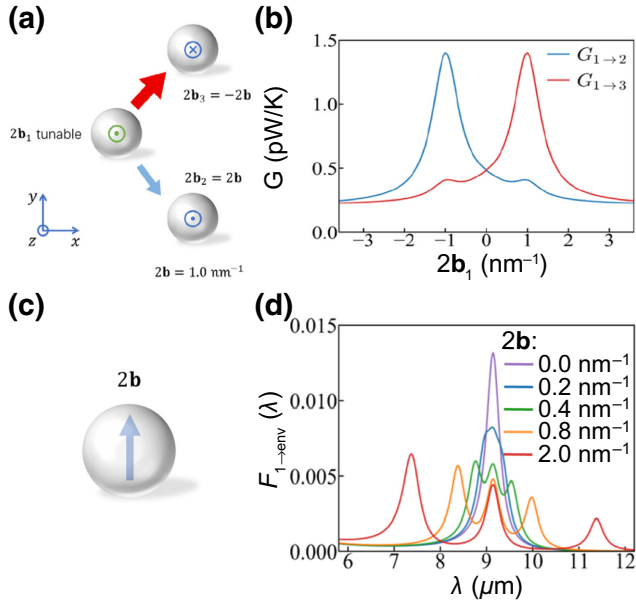


FIG. 11. Thermal router using magnetic Weyl semimetal. (a) Schematic of a thermal router consisting of three same-sized magnetic Weyl semimetal nanospheres forming an isosceles triangle with a leg length of 320 nm, a base length of 554 nm, and a vertex angle of  $120^\circ$ . In sphere 1, the Weyl node separation,  $2b_1$ , is along the  $z$  direction and can be controlled by an external field. The Weyl node separations in spheres 2 and 3 are fixed at  $2b_2 = 1.0 \text{ nm}^{-1}$  and  $2b_3 = -1.0 \text{ nm}^{-1}$  along the  $z$  direction, respectively [185]. (b) Thermal conductance  $G_{1 \rightarrow 2}$  and  $G_{2 \rightarrow 1}$  as a function of  $2b_1$  [185]. (c) Schematic of a magnetic Weyl semimetal sphere with a radius of 100 nm. Weyl node separation is  $2b$  [185]. (d) Spectra of transmission coefficient from the sphere in (c) to the environment at different values of  $2b$  [185].

for many-body radiative heat transfer [186]. For example, radiative heat transfer is reciprocal in a linear chain of magneto-optical nanospheres under a uniform external magnetic field [183] and in a cluster of identical magneto-optical spheres with centers on a plane and with local magnetization parallel to the plane [176,186].

On the other hand, for radiative heat transfer in a time-invariant linear two-body system, the overall radiative heat transfer between the two bodies is reciprocal, as required by the second law of thermodynamics. However, in two-body systems involving magneto-optical or magnetic materials, there may exist nonreciprocal radiative transfer for certain channels, for example, among different parallel wavevectors for radiative heat transfer between two plates involving magneto-optical materials [187,188]. It is shown that such nonreciprocal heat transfer for different parallel wavevectors can be used in combination with a nonreciprocal photon-occupation number in drift-current-biased graphene to achieve near-field active cooling [189].

## VII. REMARKS AND OUTLOOK

We end the review with a few remarks. Breaking Lorentz reciprocity reveals unique opportunities for controlling thermal radiation and radiative heat transfer, with great potential for fundamentally improving a broad range of photonic energy-conversion technologies and thermal management. Despite great progress in nonreciprocal emitters and absorbers, existing designs are largely limited by narrow bandwidth, small angular range, and single polarization. We provide here remarks on the challenges and opportunities. First, nonreciprocal emitters and absorbers typically operate over a narrow bandwidth [137,139–141]. Broadband reciprocal thermal emission is achieved by using metamaterials and metasurfaces [8,190]. Dual-band nonreciprocal emitters are designed using gratings and multilayers [145,191]. Related strategies may be used to achieve broadband nonreciprocal emitters. Second, nonreciprocal emission typically takes place at rather large angles [137,139–141]. Recently, the concept of topology [150] is used to broaden the angular range of nonreciprocal emitters. Specifically, topological phase singular pairs are used to investigate nonreciprocal emitters by tuning material loss and radiative loss [150], leading to nonreciprocal emission at a wider angular range. Third, existing nonreciprocal emitter designs [137,139–141] only work for TM polarization, while the emission and absorption at TE polarization are reciprocal. For potential application of nonreciprocal emitters and absorbers in energy conversion, such as solar cells [19,98], harvesting outgoing radiation [20,22], thermophotovoltaics [20], and in thermal management, achieving nonreciprocal emission and absorption in both polarizations is desired. To approach the Landsberg limit using semitransparent nonreciprocal multijunction solar cells, it is indicated that one way to harvest both polarizations of incoming sunlight is to convert the TE polarization to TM polarization and harvest the converted light in two separate sets of nonreciprocal solar cells [98]. The polarization conversion can be achieved by combining a polarization splitter, and subsequently, a polarization rotator. A compact design of nonreciprocal emitters for both polarizations is desirable, and more research is needed in this direction.

Experiments on nonreciprocal thermal photonics are lacking, regardless of the mechanisms used for breaking the Lorentz reciprocity. First, one challenge for experimentally achieving nonreciprocal emission and absorption using magneto-optical materials is the requirement for a relatively large magnetic field of about a few T [137,192] or a narrow bandwidth [141]. To this end, magnetic Weyl semimetals, such as  $\text{Co}_3\text{Sn}_2\text{S}_2$  [133,134],  $\text{Co}_2\text{MnGa}$  [132],  $\text{Co}_2\text{MnAl}$  [135], and  $\text{Mn}_3\text{Sn}$  [136], are attractive as they can break the Lorentz reciprocity without an external magnetic field, and thus, are promising for nonreciprocal thermal photonic applications without an external

magnetic field. In particular, magnetic Weyl semimetals, such as  $\text{Co}_2\text{MnGa}$  [132] and  $\text{Co}_2\text{MnAl}$  [135] with high Curie temperatures (726 K for  $\text{Co}_2\text{MnAl}$  [193] and 690 K for  $\text{Co}_2\text{MnGa}$  [132]), and  $\text{Mn}_3\text{Sn}$  [136] with a Neel temperature of 430 K, could be useful for experiments at above room temperature. Second, for nonreciprocal energy conversion and heat transfer based on time modulation, modulation with a high bandwidth, large amplitude, and low power consumption is needed. In particular, a modulator integrated with graphene achieves an intrinsic modulation speed of 150 GHz [164]. Such a modulation speed is about 2 orders of magnitude smaller than the frequency of thermal radiation at 300 K, therefore, making time modulation relevant for achieving nonreciprocal thermal emission. Third, for many phenomena of nonreciprocal near-field radiative heat transfer, the characteristic feature is typically small as a few pW/K. The recent advances in high-precision nanocalorimetry and scanning thermal microscopy [25,26,30–32,71,194–199] could be useful for experimentally verifying predicted effects. Fourth, nonlinear radiative heat transfer could have the potential to control heat flow. A rigorous calculation of nonlinear radiative heat transfer based on fluctuational electrodynamics [175] would be useful but challenging. Experiments on nonlinear radiative heat transfer are needed to verify the predictions of heat extraction [173,174].

With the rich phenomena and advances in both theory and experiments, the field of nonreciprocal thermal photonics can have a big impact on fundamental advances and technological applications. Nonreciprocal emitters and absorbers point to fundamentally different ways of controlling thermal emission and absorption by separately controlling the two processes. Also, nonreciprocal emitters and absorbers provide opportunities for applications such as improving energy conversion in solar cells [19, 21,98], thermophotovoltaics [20], and for harvesting outgoing thermal radiation [20]; communication systems that decouple emission and absorption [159]; and thermal management. Finally, radiative heat transfer in nonreciprocal materials not only highlights the intriguing phenomenon of heat flow [91,178,179] but also points to applications such as thermal routers [185], thermal diodes [180–182], and thermal magnetometry [178,183].

### ACKNOWLEDGMENTS

This work is supported by the Charles E. Kaufman Foundation, a supporting organization of the Pittsburgh Foundation, and by the start-up funding supported by the Pennsylvania State University.

The authors declare no competing financial interests.

[1] S. H. Fan, Thermal photonics and energy applications, *Joule* **1**, 264 (2017).

[2] W. Li and S. H. Fan, Nanophotonic control of thermal radiation for energy applications, *Opt. Express* **26**, 15995 (2018).

[3] Y. Li, W. Li, T. C. Han, X. Zheng, J. X. Li, B. W. Li, S. H. Fan, and C. W. Qiu, Transforming heat transfer with thermal metamaterials and devices, *Nat. Rev. Mater.* **6**, 488 (2021).

[4] M. Laroche, R. Carminati, and J. J. Greffet, Coherent Thermal Antenna Using a Photonic Crystal Slab, *Phys. Rev. Lett.* **96**, 123903 (2006).

[5] V. Rinnerbauer, Y. X. Yeng, W. R. Chan, J. J. Senkevich, J. D. Joannopoulos, M. Soljacic, and I. Celanovic, High-temperature stability and selective thermal emission of polycrystalline tantalum photonic crystals, *Opt. Express* **21**, 11482 (2013).

[6] K. A. Arpin, M. D. Losego, A. N. Cloud, H. Ning, J. Mallek, N. P. Sergeant, L. Zhu, Z. Yu, B. Kalanyan, G. N. Parsons, *et al.*, Three-dimensional self-assembled photonic crystals with high temperature stability for thermal emission modification, *Nat. Commun.* **4**, 2630 (2013).

[7] T. Inoue, M. De Zoysa, T. Asano, and S. Noda, Realization of dynamic thermal emission control, *Nat. Mater.* **13**, 928 (2014).

[8] X. L. Liu, T. Tyler, T. Starr, A. F. Starr, N. M. Jokerst, and W. J. Padilla, Taming the Blackbody with Infrared Metamaterials as Selective Thermal Emitters, *Phys. Rev. Lett.* **107**, 045901 (2011).

[9] M. A. Kats, R. Blanchard, S. Y. Zhang, P. Genevet, C. H. Ko, S. Ramanathan, and F. Capasso, Vanadium dioxide as a natural disordered metamaterial: Perfect thermal emission and large broadband negative differential thermal emittance, *Phys. Rev. X* **3**, 041004 (2013).

[10] P. N. Dyachenko, S. Molesky, A. Y. Petrov, M. Storer, T. Krekel, S. Lang, M. Ritter, Z. Jacob, and M. Eich, Controlling thermal emission with refractory epsilon-near-zero metamaterials via topological transitions, *Nat. Commun.* **7**, 11809 (2016).

[11] M. Zhou, E. Khoram, D. J. Liu, B. Y. Liu, S. H. Fan, M. L. Povinelli, and Z. F. Yu, Self-focused thermal emission and holography realized by mesoscopic thermal emitters, *ACS Photonics* **8**, 497 (2021).

[12] A. C. Overvig, S. A. Mann, and A. Alu, Thermal metasurfaces: Complete emission control by combining local and nonlocal light-matter interactions, *Phys. Rev. X* **11**, 021050 (2021).

[13] J. J. Greffet, R. Carminati, K. Joulain, J. P. Mulet, S. P. Mainguy, and Y. Chen, Coherent emission of light by thermal sources, *Nature* **416**, 61 (2002).

[14] G. Barbillon, E. Sakat, J. P. Hugonin, S. A. Biehs, and P. Ben-Abdallah, True thermal antenna with hyperbolic metamaterials, *Opt. Express* **25**, 23356 (2017).

[15] G. Kirchhoff, Ueber das Verhältniss zwischen dem Emissionsvermögen und dem Absorptionsvermögen der Körper für Wärme und Licht, *Ann. Phys.* **185**, 275 (1860).

[16] R. Siegel and J. Howell, *Thermal Radiation Heat Transfer*, 4th ed. (Taylor & Francis, London, 2001).

[17] T. L. Bergman, F. P. Incropera, D. P. Dewitt, and A. S. Lavine, *Fundamentals of Heat and Mass Transfer* (Wiley, Hoboken, 2011).

[18] M. Planck, *The Theory of Heat Radiation* (Dover Publications, New York, 2013).

- [19] M. A. Green, Time-asymmetric photovoltaics, *Nano Lett.* **12**, 5985 (2012).
- [20] S. Buddhiraju, P. Santhanam, and S. H. Fan, Thermodynamic limits of energy harvesting from outgoing thermal radiation, *Proc. Natl. Acad. Sci. U. S. A.* **115**, E3609 (2018).
- [21] H. Ries, Complete and reversible absorption of radiation, *Appl. Phys. B* **32**, 153 (1983).
- [22] W. Li, S. Buddhiraju, and S. Fan, Thermodynamic limits for simultaneous energy harvesting from the hot sun and cold outer space, *Light: Sci. Appl.* **9**, 68 (2020).
- [23] W. C. Snyder, Z. M. Wan, and X. W. Li, Thermodynamic constraints on reflectance reciprocity and Kirchhoff's law, *Appl. Opt.* **37**, 3464 (1998).
- [24] C. Khandekar, F. Khosravi, Z. Li, and Z. Jacob, New spin-resolved thermal radiation laws for nonreciprocal bianisotropic media, *New J. Phys.* **22**, 123005 (2020).
- [25] S. Shen, A. Narayanaswamy, and G. Chen, Surface phonon polaritons mediated energy transfer between nanoscale gaps, *Nano Lett.* **9**, 2909 (2009).
- [26] E. Rousseau, A. Siria, G. Jourdan, S. Volz, F. Comin, J. Chevrier, and J.-J. Greffet, Radiative heat transfer at the nanoscale, *Nat. Photonics* **3**, 514 (2009).
- [27] R. S. Ottens, V. Quetschke, S. Wise, A. A. Alemi, R. Lundock, G. Mueller, D. H. Reitze, D. B. Tanner, and B. F. Whiting, Near-Field Radiative Heat Transfer between Macroscopic Planar Surfaces, *Phys. Rev. Lett.* **107**, 014301 (2011).
- [28] R. St-Gelais, B. Guha, L. X. Zhu, S. H. Fan, and M. Lipson, Demonstration of strong near-field radiative heat transfer between integrated nanostructures, *Nano Lett.* **14**, 6971 (2014).
- [29] B. Song, Y. Ganjeh, S. Sadat, D. Thompson, A. Fiorino, V. Fernandez-Hurtado, J. Feist, F. J. Garcia-Vidal, J. C. Cuevas, P. Reddy, *et al.*, Enhancement of near-field radiative heat transfer using polar dielectric thin films, *Nat. Nanotechnol.* **10**, 253 (2015).
- [30] B. Song, D. Thompson, A. Fiorino, Y. Ganjeh, P. Reddy, and E. Meyhofer, Radiative heat conductances between dielectric and metallic parallel plates with nanoscale gaps, *Nat. Nanotechnol.* **11**, 509 (2016).
- [31] R. St-Gelais, L. X. Zhu, S. H. Fan, and M. Lipson, Near-field radiative heat transfer between parallel structures in the deep subwavelength regime, *Nat. Nanotechnol.* **11**, 515 (2016).
- [32] J. I. Watjen, B. Zhao, and Z. M. Zhang, Near-field radiative heat transfer between doped-Si parallel plates separated by a spacing down to 200 nm, *Appl. Phys. Lett.* **109**, 203112 (2016).
- [33] M. P. Bernardi, D. Milovich, and M. Francoeur, Radiative heat transfer exceeding the blackbody limit between macroscale planar surfaces separated by a nanosize vacuum gap, *Nat. Commun.* **7**, 12900 (2016).
- [34] J. DeSutter, L. Tang, and M. Francoeur, A near-field radiative heat transfer device, *Nat. Nanotechnol.* **14**, 751 (2019).
- [35] A. Fiorino, D. Thompson, L. X. Zhu, B. Song, P. Reddy, and E. Meyhofer, Giant enhancement in radiative heat transfer in sub-30 nm gaps of plane parallel surfaces, *Nano Lett.* **18**, 3711 (2018).
- [36] M. Lim, J. Song, S. S. Lee, and B. J. Lee, Tailoring near-field thermal radiation between metallo-dielectric multilayers using coupled surface plasmon polaritons, *Nat. Commun.* **9**, 4302 (2018).
- [37] M. Ghashami, H. Y. Geng, T. Kim, N. Iacopino, S. K. Cho, and K. Park, Precision Measurement of Phonon-Polaritonic Near-Field Energy Transfer between Macroscale Planar Structures Under Large Thermal Gradients, *Phys. Rev. Lett.* **120**, 175901 (2018).
- [38] J. Yang, W. Du, Y. S. Su, Y. Fu, S. X. Gong, S. L. He, and Y. G. Ma, Observing of the super-Planckian near-field thermal radiation between graphene sheets, *Nat. Commun.* **9**, 4033 (2018).
- [39] H. Salihoglu, W. Nam, L. Traverso, M. Segovia, P. K. Venuthurumilli, W. Liu, Y. Wei, W. J. Li, and X. F. Xu, Near-field thermal radiation between two plates with sub-10 nm vacuum separation, *Nano Lett.* **20**, 6091 (2020).
- [40] S. A. Biehs, R. Messina, P. S. Venkataram, A. W. Rodriguez, J. C. Cuevas, and P. Ben-Abdallah, Near-field radiative heat transfer in many-body systems, *Rev. Mod. Phys.* **93**, 025009 (2021).
- [41] A. V. Shchegrov, K. Joulain, R. Carminati, and J. J. Greffet, Near-Field Spectral Effects due to Electromagnetic Surface Excitations, *Phys. Rev. Lett.* **85**, 1548 (2000).
- [42] M. Francoeur, M. P. Menguc, and R. Vaillon, Spectral tuning of near-field radiative heat flux between two thin silicon carbide films, *J. Phys. D: Appl. Phys.* **43**, 075501 (2010).
- [43] P. Sabbaghi, L. S. Long, X. Y. Ying, L. Lambert, S. Taylor, C. Messner, and L. P. Wang, Super-Planckian radiative heat transfer between macroscale metallic surfaces due to near-field and thin-film effects, *J. Appl. Phys.* **128**, 025305 (2020).
- [44] M. Lim, J. Song, S. S. Lee, J. Lee, and B. J. Lee, Surface-Plasmon-Enhanced Near-Field Radiative Heat Transfer between Planar Surfaces with a Thin-Film Plasmonic Coupler, *Phys. Rev. Appl.* **14**, 014070 (2020).
- [45] O. D. Miller, S. G. Johnson, and A. W. Rodriguez, Effectiveness of Thin Films in Lieu of Hyperbolic Metamaterials in the Near Field, *Phys. Rev. Lett.* **112**, 157402 (2014).
- [46] V. Fernandez-Hurtado, F. J. Garcia-Vidal, S. H. Fan, and J. C. Cuevas, Enhancing Near-Field Radiative Heat Transfer with Si-Based Metasurfaces, *Phys. Rev. Lett.* **118**, 203901 (2017).
- [47] X. L. Liu and Z. M. Zhang, Near-field thermal radiation between metasurfaces, *ACS Photonics* **2**, 1320 (2015).
- [48] Y. Yang and L. P. Wang, Spectrally Enhancing Near-Field Radiative Transfer between Metallic Gratings by Exciting Magnetic Polaritons in Nanometric Vacuum Gaps, *Phys. Rev. Lett.* **117**, 044301 (2016).
- [49] J. Dai, S. A. Dyakov, S. I. Bozhevolnyi, and M. Yan, Near-field radiative heat transfer between metasurfaces: A full-wave study based on two-dimensional grooved metal plates, *Phys. Rev. B* **94**, 125431 (2016).
- [50] C. Y. Luo, A. Narayanaswamy, G. Chen, and J. D. Joannopoulos, Thermal Radiation from Photonic Crystals: A Direct Calculation, *Phys. Rev. Lett.* **93**, 213905 (2004).
- [51] A. W. Rodriguez, O. Ilic, P. Bermel, I. Celanovic, J. D. Joannopoulos, M. Soljacic, and S. G. Johnson, Frequency-Selective Near-Field Radiative Heat Transfer between



- Photonic Crystal Slabs: A Computational Approach for Arbitrary Geometries and Materials, *Phys. Rev. Lett.* **107**, 114302 (2011).
- [52] O. Ilic, M. Jablan, J. D. Joannopoulos, I. Celanovic, H. Buljan, and M. Soljacic, Near-field thermal radiation transfer controlled by plasmons in graphene, *Phys. Rev. B* **85**, 155422 (2012).
- [53] C. L. Zhou, X. H. Wu, Y. Zhang, and H. L. Yi, Super-Planckian thermal radiation in borophene sheets, *Int. J. Heat Mass Transfer* **183**, 122140 (2022).
- [54] N. H. Thomas, M. C. Sherrott, J. Broulliet, H. A. Atwater, and A. J. Minnich, Electronic modulation of near-field radiative transfer in graphene field effect heterostructures, *Nano Lett.* **19**, 3898 (2019).
- [55] B. Zhao, B. Guizal, Z. M. M. Zhang, S. H. Fan, and M. Antezza, Near-field heat transfer between graphene/hBN multilayers, *Phys. Rev. B* **95**, 9 (2017).
- [56] Y. Zhang, H. L. Yi, and H. P. Tan, Near-field radiative heat transfer between black phosphorus sheets via anisotropic surface plasmon polaritons, *ACS Photonics* **5**, 3739 (2018).
- [57] S. A. Biehs, M. Tschikin, and P. Ben-Abdallah, Hyperbolic Metamaterials as an Analog of a Blackbody in the Near Field, *Phys. Rev. Lett.* **109**, 104301 (2012).
- [58] Y. Guo, C. L. Cortes, S. Molesky, and Z. Jacob, Broadband super-Planckian thermal emission from hyperbolic metamaterials, *Appl. Phys. Lett.* **101**, 131106 (2012).
- [59] R. S. DiMatteo, P. Greiff, S. L. Finberg, K. A. Young-Waithe, H. K. H. Choy, M. M. Masaki, and C. G. Fonstad, Enhanced photogeneration of carriers in a semiconductor via coupling across a nonisothermal nanoscale vacuum gap, *Appl. Phys. Lett.* **79**, 1894 (2001).
- [60] A. Narayanaswamy and G. Chen, Surface modes for near field thermophotovoltaics, *Appl. Phys. Lett.* **82**, 3544 (2003).
- [61] K. Park, S. Basu, W. P. King, and Z. M. Zhang, Performance analysis of near-field thermophotovoltaic devices considering absorption distribution, *J. Quant. Spectrosc. Radiat. Transfer* **109**, 305 (2008).
- [62] A. Fiorino, L. X. Zhu, D. Thompson, R. Mittapally, P. Reddy, and E. Meyhofer, Nanogap near-field thermophotovoltaics, *Nat. Nanotechnol.* **13**, 806 (2018).
- [63] T. Inoue, T. Koyama, D. D. Kang, K. Ikeda, T. Asano, and S. Noda, One-chip near-field thermophotovoltaic device integrating a thin-film thermal emitter and photovoltaic cell, *Nano Lett.* **19**, 3948 (2019).
- [64] G. R. Bhatt, B. Zhao, S. Roberts, I. Datta, A. Mohanty, T. Lin, J. M. Hartmann, R. St-Gelais, S. H. Fan, and M. Lipson, Integrated near-field thermo-photovoltaics for heat recycling, *Nat. Commun.* **11**, 2545 (2020).
- [65] R. Mittapally, B. Lee, L. Zhu, A. Reihani, J. W. Lim, D. Fan, S. R. Forrest, P. Reddy, and E. Meyhofer, Near-field thermophotovoltaics for efficient heat to electricity conversion at high power density, *Nat. Commun.* **12**, 4364 (2021).
- [66] C. Lucchesi, D. Cakiroglu, J. P. Perez, T. Taliercio, E. Tourmie, P. O. Chapuis, and R. Vaillon, Near-field thermophotovoltaic conversion with high electrical power density and cell efficiency above 14%, *Nano Lett.* **21**, 4524 (2021).
- [67] K. F. Chen, P. Santhanam, S. Sandhu, L. X. Zhu, and S. H. Fan, Heat-flux control and solid-state cooling by regulating chemical potential of photons in near-field electromagnetic heat transfer, *Phys. Rev. B* **91**, 134301 (2015).
- [68] X. L. Liu and Z. M. M. Zhang, High-performance electroluminescent refrigeration enabled by photon tunneling, *Nano Energy* **26**, 353 (2016).
- [69] K. F. Chen, P. Santhanam, and S. H. Fan, Near-Field Enhanced Negative Luminescent Refrigeration, *Phys. Rev. Appl.* **6**, 024014 (2016).
- [70] K. F. Chen, T. Y. P. Xiao, P. Santhanam, E. Yablonovitch, and S. H. Fan, High-performance near-field electroluminescent refrigeration device consisting of a GaAs light emitting diode and a Si photovoltaic cell, *J. Appl. Phys.* **122**, 143104 (2017).
- [71] L. Zhu, A. Fiorino, D. Thompson, R. Mittapally, E. Meyhofer, and P. Reddy, Near-field photonic cooling through control of the chemical potential of photons, *Nature* **566**, 239 (2019).
- [72] C. R. Otey, W. T. Lau, and S. H. Fan, Thermal Rectification through Vacuum, *Phys. Rev. Lett.* **104**, 154301 (2010).
- [73] P. Ben-Abdallah and S. A. Biehs, Phase-change radiative thermal diode, *Appl. Phys. Lett.* **103**, 191907 (2013).
- [74] L. X. Zhu, C. R. Otey, and S. H. Fan, Ultrahigh-contrast and large-bandwidth thermal rectification in near-field electromagnetic thermal transfer between nanoparticles, *Phys. Rev. B* **88**, 184301 (2013).
- [75] K. Ito, K. Nishikawa, H. Iizuka, and H. Toshiyoshi, Experimental investigation of radiative thermal rectifier using vanadium dioxide, *Appl. Phys. Lett.* **105**, 253503 (2014).
- [76] A. Fiorino, D. Thompson, L. X. Zhu, R. Mittapally, S. A. Biehs, O. Bezenenet, N. El-Bondry, S. Bansropun, P. Ben-Abdallah, E. Meyhofer, *et al.*, A thermal diode based on nanoscale thermal radiation, *ACS Nano* **12**, 5774 (2018).
- [77] A. Ghanekar, Y. P. Tian, M. Ricci, S. N. Zhang, O. Gregory, and Y. Zheng, Near-field thermal rectification devices using phase change periodic nanostructure, *Opt. Express* **26**, A209 (2018).
- [78] Q. Z. Li, H. Y. He, Q. Chen, and B. Song, Thin-Film Radiative Thermal Diode with Large Rectification, *Phys. Rev. Appl.* **16**, 014069 (2021).
- [79] E. Moncada-Villa and J. C. Cuevas, Normal-Metal-Superconductor Near-Field Thermal Diodes and Transistors, *Phys. Rev. Appl.* **15**, 024036 (2021).
- [80] D. D. Feng, S. K. Yee, and Z. M. M. Zhang, Near-field photonic thermal diode based on hBN and InSb films, *Appl. Phys. Lett.* **119**, 181111 (2021).
- [81] L. P. Wang and Z. M. Zhang, Thermal rectification enabled by near-field radiative heat transfer between intrinsic silicon and a dissimilar material, *Nanoscale Microscale Thermophys. Eng.* **17**, 337 (2013).
- [82] Q. Z. Li, Q. Chen, and B. Song, Giant radiative thermal rectification using an intrinsic semiconductor film, *Mater. Today Phys.* **23**, 100632 (2022).
- [83] P. Ben-Abdallah and S. A. Biehs, Near-Field Thermal Transistor, *Phys. Rev. Lett.* **112**, 044301 (2014).



- [84] J. Ordonez-Miranda, Y. Ezzahri, J. Drevillon, and K. Joulain, Transistorlike Device for Heating and Cooling Based on the Thermal Hysteresis of VO<sub>2</sub>, *Phys. Rev. Appl.* **6**, 054003 (2016).
- [85] I. Latella, O. Marconot, J. Sylvestre, L. G. Frechette, and P. Ben-Abdallah, Dynamical Response of a Radiative Thermal Transistor Based on Suspended Insulator-Metal-Transition Membranes, *Phys. Rev. Appl.* **11**, 024004 (2019).
- [86] G. T. Papadakis, B. Zhao, S. Buddhiraju, and S. H. Fan, Gate-tunable near-field heat transfer, *ACS Photonics* **6**, 709 (2019).
- [87] D. Thompson, L. X. Zhu, E. Meyhofer, and P. Reddy, Nanoscale radiative thermal switching via multi-body effects, *Nat. Nanotechnol.* **15**, 99 (2020).
- [88] J. B. Peng, G. M. Tang, L. Q. Wang, R. Macedo, H. Chen, and J. Ren, Twist-induced near-field thermal switch using nonreciprocal surface magnon-polaritons, *ACS Photonics* **8**, 2183 (2021).
- [89] W. A. Challener, C. B. Peng, A. V. Itagi, D. Karns, W. Peng, Y. Y. Peng, X. M. Yang, X. B. Zhu, N. J. Gokemeijer, Y. T. Hsia, *et al.*, Heat-assisted magnetic recording by a near-field transducer with efficient optical energy transfer, *Nat. Photonics* **3**, 220 (2009).
- [90] J. B. Pendry, Radiative exchange of heat between nanostructures, *J. Phys.: Condens. Matter* **11**, 6621 (1999).
- [91] L. X. Zhu and S. H. Fan, Persistent Directional Current at Equilibrium in Nonreciprocal Many-Body Near Field Electromagnetic Heat Transfer, *Phys. Rev. Lett.* **117**, 134303 (2016).
- [92] W. Shockley and H. J. Queisser, Detailed balance limit of efficiency of *p-n* junction solar cells, *J. Appl. Phys.* **32**, 510 (1961).
- [93] H. Pauwels and A. Devos, Determination of the maximum efficiency solar-cell structure, *Solid-State Electron.* **24**, 835 (1981).
- [94] A. Marti and G. L. Araujo, Limiting efficiencies for photovoltaic energy conversion in multigap systems, *Sol. Energy Mater. Sol. Cells* **43**, 203 (1996).
- [95] A. S. Brown and M. A. Green, Limiting efficiency for current-constrained two-terminal tandem cell stacks, *Prog. Photovoltaics* **10**, 299 (2002).
- [96] P. T. Landsberg and G. Tonge, Thermodynamic energy-conversion efficiencies, *J. Appl. Phys.* **51**, R1 (1980).
- [97] A. Pusch, J. M. Gordon, A. Mellor, J. J. Krich, and N. J. Ekins-Daukes, Fundamental Efficiency Bounds for the Conversion of a Radiative Heat Engine's Own Emission into Work, *Phys. Rev. Appl.* **12**, 064018 (2019).
- [98] Y. B. Park, B. Zhao, and S. H. Fan, Reaching the ultimate efficiency of solar energy harvesting with a nonreciprocal multijunction solar cell, *Nano Lett.* **22**, 448 (2022).
- [99] Y. Park, V. S. Asadchy, B. Zhao, C. Guo, J. H. Wang, and S. H. Fan, Violating Kirchhoff's law of thermal radiation in semitransparent structures, *ACS Photonics* **8**, 2417 (2021).
- [100] S. J. Byrnes, R. Blanchard, and F. Capasso, Harvesting renewable energy from Earth's mid-infrared emissions, *Proc. Natl. Acad. Sci. U. S. A.* **111**, 3927 (2014).
- [101] F. Trombe, Perspectives sur l'utilisation des rayonnements solaires et terrestres dans certaines régions du monde, *Rev. Gen. Therm.* **6**, 1285 (1967).
- [102] S. Catalanotti, V. Cuomo, G. Piro, D. Ruggi, V. Silvestrini, and G. Troise, The radiative cooling of selective surfaces, *Sol. Energy* **17**, 83 (1975).
- [103] B. Bartoli, S. Catalanotti, B. Coluzzi, V. Cuomo, V. Silvestrini, and G. Troise, Nocturnal and diurnal performances of selective radiators, *Appl. Energy* **3**, 267 (1977).
- [104] A. W. Harrison and M. R. Walton, Radiative cooling of TiO<sub>2</sub> white paint, *Sol. Energy* **20**, 185 (1978).
- [105] C. G. Granqvist and A. Hjortsberg, Radiative cooling to low-temperatures: General considerations and application to selectively emitting SiO films, *J. Appl. Phys.* **52**, 4205 (1981).
- [106] P. Berdahl, Radiative cooling with MgO and or LiF layers, *Appl. Opt.* **23**, 370 (1984).
- [107] C. G. Granqvist, Radiative heating and cooling with spectrally selective surfaces, *Appl. Opt.* **20**, 2606 (1981).
- [108] A. R. Gentle and G. B. Smith, Radiative heat pumping from the Earth using surface phonon resonant nanoparticles, *Nano Lett.* **10**, 373 (2010).
- [109] C. G. Granqvist and A. Hjortsberg, Letter to the editor, *Sol. Energy* **24**, 216 (1980).
- [110] C. G. Granqvist and A. Hjortsberg, Surfaces for radiative cooling: Silicon monoxide films on aluminum, *Appl. Phys. Lett.* **36**, 139 (1980).
- [111] L. X. Zhu, A. P. Raman, and S. H. Fan, Radiative cooling of solar absorbers using a visibly transparent photonic crystal thermal blackbody, *Proc. Natl. Acad. Sci. U. S. A.* **112**, 12282 (2015).
- [112] N. N. Shi, C. C. Tsai, F. Camino, G. D. Bernard, N. F. Yu, and R. Wehner, Keeping cool: Enhanced optical reflection and radiative heat dissipation in Saharan silver ants, *Science* **349**, 298 (2015).
- [113] M. M. Hossain, B. H. Jia, and M. Gu, A metamaterial emitter for highly efficient radiative cooling, *Adv. Opt. Mater.* **3**, 1047 (2015).
- [114] A. R. Gentle and G. B. Smith, A subambient open roof surface under the mid-summer sun, *Adv. Sci.* **2**, 1500119 (2015).
- [115] A. P. Raman, M. A. Anoma, L. Zhu, E. Rephaeli, and S. Fan, Passive radiative cooling below ambient air temperature under direct sunlight, *Nature* **515**, 540 (2014).
- [116] Z. Chen, L. X. Zhu, A. Raman, and S. H. Fan, Radiative cooling to deep sub-freezing temperatures through a 24-h day-night cycle, *Nat. Commun.* **7**, 13729 (2016).
- [117] Y. Zhai, Y. G. Ma, S. N. David, D. L. Zhao, R. N. Lou, G. Tan, R. G. Yang, and X. B. Yin, Scalable-manufactured randomized glass-polymer hybrid metamaterial for daytime radiative cooling, *Science* **355**, 1062 (2017).
- [118] T. Li, Y. Zhai, S. M. He, W. T. Gan, Z. Y. Wei, M. Heidarinejad, D. Dalgo, R. Y. Mi, X. P. Zhao, J. W. Song, *et al.*, A radiative cooling structural material, *Science* **364**, 760 (2019).
- [119] Y. Zhou, H. M. Song, J. W. Liang, M. Singer, M. Zhou, E. Stengenburgs, N. Zhang, C. Xu, T. Ng, Z. F. Yu, *et al.*, A polydimethylsiloxane-coated metal structure for all-day radiative cooling, *Nat. Sustain.* **2**, 718 (2019).
- [120] D. Li, X. Liu, W. Li, Z. H. Lin, B. Zhu, Z. Z. Li, J. L. Li, B. Li, S. H. Fan, J. W. Xie, *et al.*, Scalable and hierarchically designed polymer film as a selective thermal

- emitter for high-performance all-day radiative cooling, *Nat. Nanotechnol.* **16**, 153 (2021).
- [121] M. Zhou, H. Song, X. Xu, A. Shahsafi, Y. Qu, Z. Xia, Z. Ma, M. A. Kats, J. Zhu, B. S. Ooi, *et al.*, Vapor condensation with daytime radiative cooling, *Proc. Natl. Acad. Sci. U. S. A.* **118**, e2019292118 (2021).
- [122] Z. Chen, L. X. Zhu, W. Li, and S. H. Fan, Simultaneously and synergistically harvest energy from the Sun and outer space, *Joule* **3**, 101 (2019).
- [123] P. Santhanam and S. H. Fan, Thermal-to-electrical energy conversion by diodes under negative illumination, *Phys. Rev. B* **93**, 161410 (2016).
- [124] A. P. Raman, W. Li, and S. H. Fan, Generating light from darkness, *Joule* **3**, 2679 (2019).
- [125] M. Ono, P. Santhanam, W. Li, B. Zhao, and S. H. Fan, Experimental demonstration of energy harvesting from the sky using the negative illumination effect of a semiconductor photodiode, *Appl. Phys. Lett.* **114**, 161102 (2019).
- [126] C. W. Lin, B. N. Wang, K. H. Teo, and Z. M. Zhang, Performance comparison between photovoltaic and thermoradiative devices, *J. Appl. Phys.* **122**, 243103 (2017).
- [127] S. Ahmed, Z. P. Li, M. S. Javed, and T. Ma, A review on the integration of radiative cooling and solar energy harvesting, *Mater. Today Energy* **21**, 100776 (2021).
- [128] D. Jalas, A. Petrov, M. Eich, W. Freude, S. H. Fan, Z. F. Yu, R. Baets, M. Popovic, A. Melloni, J. D. Joannopoulos, *et al.*, What is—and what is not—an optical isolator, *Nat. Photonics* **7**, 579 (2013).
- [129] S. H. Fan, R. Baets, A. Petrov, Z. F. Yu, J. D. Joannopoulos, W. Freude, A. Melloni, M. Popovic, M. Vanwolleghem, D. Jalas, *et al.*, Comment on “Nonreciprocal light propagation in a silicon photonic circuit”, *Science* **335**, 38 (2012).
- [130] K. Seeger, *Semiconductor Physics: An Introduction*, 9th ed., Advanced Texts in Physics (Springer, Berlin, Heidelberg, 2004).
- [131] Rayleigh, On the magnetic rotation of light and the second law of thermo dynamics, *Nature* **64**, 577 (1901).
- [132] I. Belopolski, K. Manna, D. S. Sanchez, G. Q. Chang, B. Ernst, J. X. Yin, S. S. Zhang, T. Cochran, N. Shumiya, H. Zheng, *et al.*, Discovery of topological Weyl fermion lines and drumhead surface states in a room temperature magnet, *Science* **365**, 1278 (2019).
- [133] D. F. Liu, A. J. Liang, E. K. Liu, Q. N. Xu, Y. W. Li, C. Chen, D. Pei, W. J. Shi, S. K. Mo, P. Dudin, *et al.*, Magnetic Weyl semimetal phase in a Kagome crystal, *Science* **365**, 1282 (2019).
- [134] N. Morali, R. Batabyal, P. K. Nag, E. K. Liu, Q. A. Xu, Y. Sun, B. H. Yan, C. Felser, N. Avraham, and H. Beidenkopf, Fermi-arc diversity on surface terminations of the magnetic Weyl semimetal  $\text{Co}_3\text{Sn}_2\text{S}_2$ , *Science* **365**, 1286 (2019).
- [135] P. G. Li, J. Koo, W. Ning, J. G. Li, L. X. Miao, L. J. Min, Y. L. Zhu, Y. Wang, N. Alem, C. X. Liu, *et al.*, Giant room temperature anomalous Hall effect and tunable topology in a ferromagnetic topological semimetal  $\text{Co}_2\text{MnAl}$ , *Nat. Commun.* **11**, 3476 (2020).
- [136] K. Kuroda, T. Tomita, M. T. Suzuki, C. Bareille, A. A. Nugroho, P. Goswami, M. Ochi, M. Ikhlas, M. Nakayama, S. Akebi, *et al.*, Evidence for magnetic Weyl fermions in a correlated metal, *Nat. Mater.* **16**, 1090 (2017).
- [137] L. X. Zhu and S. H. Fan, Near-complete violation of detailed balance in thermal radiation, *Phys. Rev. B* **90**, 220301(R) (2014).
- [138] Z. F. Yu, Z. Wang, and S. H. Fan, One-way total reflection with one-dimensional magneto-optical photonic crystals, *Appl. Phys. Lett.* **90**, 121133 (2007).
- [139] B. Zhao, C. Guo, C. A. C. Garcia, P. Narang, and S. H. Fan, Axion-field-enabled nonreciprocal thermal radiation in Weyl semimetals, *Nano Lett.* **20**, 1923 (2020).
- [140] Y. Tsurimaki, X. Qian, S. Pajovic, F. Han, M. D. Li, and G. Chen, Large nonreciprocal absorption and emission of radiation in type-I Weyl semimetals with time reversal symmetry breaking, *Phys. Rev. B* **101**, 165426 (2020).
- [141] B. Zhao, Y. Shi, J. H. Wang, Z. X. Zha, N. Zhao, and S. H. Fan, Near-complete violation of Kirchhoff’s law of thermal radiation with a 0.3 T magnetic field, *Opt. Lett.* **44**, 4203 (2019).
- [142] J. Wu, F. Wu, T. C. Zhao, and X. H. Wu, Tunable nonreciprocal thermal emitter based on metal grating and graphene, *Int. J. Therm. Sci.* **172**, 107316 (2022).
- [143] B. Zhao, J. H. Wang, Z. X. Zhao, C. Guo, Z. F. Yu, and S. H. Fan, Nonreciprocal Thermal Emitters Using Metasurfaces with Multiple Diffraction Channels, *Phys. Rev. Appl.* **16**, 064001 (2021).
- [144] H. Wang, Y. Z. Lei, and J. F. Han, Enhanced nonreciprocal thermal radiation properties of graphene-based magneto-optical materials, *Opt. Laser Technol.* **142**, 107279 (2021).
- [145] J. Wu, F. Wu, and X. H. Wu, Strong dual-band nonreciprocal radiation based on a four-part periodic metal grating, *Opt. Mater.* **120**, 111476 (2021).
- [146] H. Wang, H. Wu, and J. Q. Zhou, Nonreciprocal optical properties based on magneto-optical materials: *n*-InAs, GaAs and HgCdTe, *J. Quant. Spectrosc. Radiat. Transfer* **206**, 254 (2018).
- [147] H. Wang, H. Wu, and Z. Y. Shen, Nonreciprocal optical properties of thermal radiation with SiC grating magneto-optical materials, *Opt. Express* **25**, 19609 (2017).
- [148] X. H. Wu, R. Y. Liu, H. Y. Yu, and B. Y. Wu, Strong nonreciprocal radiation in magnetophotonic crystals, *J. Quant. Spectrosc. Radiat. Transfer* **272**, 107794 (2021).
- [149] J. Wu, Z. M. Wang, H. Zhai, Z. X. Shi, X. H. Wu, and F. Wu, Near-complete violation of Kirchhoff’s law of thermal radiation in ultrathin magnetic Weyl semimetal films, *Opt. Mater. Express* **11**, 4058 (2021).
- [150] M. Liu, C. Zhao, Y. Zeng, Y. Chen, C. Zhao, and C.-W. Qiu, Evolution and Nonreciprocity of Loss-Induced Topological Phase Singularity Pairs, *Phys. Rev. Lett.* **127**, 266101 (2021).
- [151] S. Pajovic, Y. Tsurimaki, X. Qian, and G. Chen, Intrinsic nonreciprocal reflection and violation of Kirchhoff’s law of radiation in planar type-I magnetic Weyl semimetal surfaces, *Phys. Rev. B* **102**, 165417 (2020).
- [152] Z. M. Zhang, X. H. Wu, and C. J. Fu, Validity of Kirchhoff’s law for semitransparent films made of anisotropic materials, *J. Quant. Spectrosc. Radiat. Transfer* **245**, 106904 (2020).
- [153] D. A. B. Miller, L. X. Zhu, and S. H. Fan, Universal modal radiation laws for all thermal emitters, *Proc. Natl. Acad. Sci. U. S. A.* **114**, 4336 (2017).

- [154] Z. F. Yu and S. H. Fan, Complete optical isolation created by indirect interband photonic transitions, *Nat. Photonics* **3**, 91 (2009).
- [155] H. Lira, Z. F. Yu, S. H. Fan, and M. Lipson, Electrically Driven Nonreciprocity Induced by Interband Photonic Transition on a Silicon Chip, *Phys. Rev. Lett.* **109**, 033901 (2012).
- [156] K. J. Fang, Z. F. Yu, and S. H. Fan, Realizing effective magnetic field for photons by controlling the phase of dynamic modulation, *Nat. Photonics* **6**, 782 (2012).
- [157] L. D. Tzuan, K. Fang, P. Nussenzveig, S. H. Fan, and M. Lipson, Non-reciprocal phase shift induced by an effective magnetic flux for light, *Nat. Photonics* **8**, 701 (2014).
- [158] E. B. Li, B. J. Eggleton, K. J. Fang, and S. H. Fan, Photonic Aharonov-Bohm effect in photon-phonon interactions, *Nat. Commun.* **5**, 3225 (2014).
- [159] Y. Hadad, J. C. Soric, and A. Alu, Breaking temporal symmetries for emission and absorption, *Proc. Natl. Acad. Sci. U. S. A.* **113**, 3471 (2016).
- [160] S. Buddhiraju, W. Li, and S. H. Fan, Photonic Refrigeration from Time-Modulated Thermal Emission, *Phys. Rev. Lett.* **124**, 077402 (2020).
- [161] H. N. Li, L. J. Fernandez-Alcazar, F. Ellis, B. Shapiro, and T. Kottos, Adiabatic Thermal Radiation Pumps for Thermal Photonics, *Phys. Rev. Lett.* **123**, 165901 (2019).
- [162] L. J. Fernandez-Alcazar, H. A. Li, M. Nafari, and T. Kottos, Implementation of optimal thermal radiation pumps using adiabatically modulated photonic cavities, *ACS Photonics* **8**, 2973 (2021).
- [163] L. J. Fernandez-Alcazar, R. Kononchuk, H. A. Li, and T. Kottos, Extreme Nonreciprocal Near-Field Thermal Radiation via Floquet Photonics, *Phys. Rev. Lett.* **126**, 204101 (2021).
- [164] C. T. Phare, Y.-H. D. Lee, J. Cardenas, and M. Lipson, Graphene electro-optic modulator with 30 GHz bandwidth, *Nat. Photonics* **9**, 511 (2015).
- [165] R. I. Epstein, M. I. Buchwald, B. C. Edwards, T. R. Gosnell, and C. E. Mungan, Observation of laser-induced fluorescent cooling of a solid, *Nature* **377**, 500 (1995).
- [166] D. V. Seletskiy, S. D. Melgaard, S. Bigotta, A. Di Lieto, M. Tonelli, and M. Sheik-Bahae, Laser cooling of solids to cryogenic temperatures, *Nat. Photonics* **4**, 161 (2010).
- [167] J. Zhang, D. H. Li, R. J. Chen, and Q. H. Xiong, Laser cooling of a semiconductor by 40 kelvin, *Nature* **493**, 504 (2013).
- [168] T. P. Xiao, K. F. Chen, P. Santhanam, S. H. Fan, and E. Yablonovitch, Electroluminescent refrigeration by ultra-efficient GaAs light-emitting diodes, *J. Appl. Phys.* **123**, 173104 (2018).
- [169] L. Fan, J. Wang, L. T. Varghese, H. Shen, B. Niu, Y. Xuan, A. M. Weiner, and M. H. Qi, An all-silicon passive optical diode, *Science* **335**, 447 (2012).
- [170] L. Fan, L. T. Varghese, J. Wang, Y. Xuan, A. M. Weiner, and M. H. Qi, Silicon optical diode with 40 dB nonreciprocal transmission, *Opt. Lett.* **38**, 1259 (2013).
- [171] K. Y. Yang, J. Skarda, M. Cotrufo, A. Dutt, G. H. Ahn, M. Sawaby, D. Vercruyse, A. Arbabian, S. H. Fan, A. Alu, *et al.*, Inverse-designed non-reciprocal pulse router for chip-based LiDAR, *Nat. Photonics* **14**, 369 (2020).
- [172] Y. Shi, Z. F. Yu, and S. H. Fan, Limitations of nonlinear optical isolators due to dynamic reciprocity, *Nat. Photonics* **9**, 388 (2015).
- [173] C. Khandekar and A. W. Rodriguez, Near-field thermal upconversion and energy transfer through a Kerr medium, *Opt. Express* **25**, 23164 (2017).
- [174] C. Khandekar, R. Messina, and A. W. Rodriguez, Near-field refrigeration and tunable heat exchange through four-wave mixing, *AIP Advances* **8**, 055029 (2018).
- [175] H. Soo and M. Kruger, Fluctuational electrodynamics for nonlinear materials in and out of thermal equilibrium, *Phys. Rev. B* **97**, 045412 (2018).
- [176] L. X. Zhu, Y. Guo, and S. H. Fan, Theory of many-body radiative heat transfer without the constraint of reciprocity, *Phys. Rev. B* **97**, 094302 (2018).
- [177] C. Guo, Y. Guo, and S. H. Fan, Relation between photon thermal Hall effect and persistent heat current in nonreciprocal radiative heat transfer, *Phys. Rev. B* **100**, 205416 (2019).
- [178] P. Ben-Abdallah, Photon Thermal Hall Effect, *Phys. Rev. Lett.* **116**, 084301 (2016).
- [179] A. Ott, S. A. Biehs, and P. Ben-Abdallah, Anomalous photon thermal Hall effect, *Phys. Rev. B* **101**, 241411 (2020).
- [180] A. Ott, R. Messina, P. Ben-Abdallah, and S. A. Biehs, Radiative thermal diode driven by nonreciprocal surface waves, *Appl. Phys. Lett.* **114**, 163105 (2019).
- [181] Y. Zhang, C. L. Zhou, H. L. Yi, and H. P. Tan, Radiative Thermal Diode Mediated by Nonreciprocal Graphene Plasmon Waveguides, *Phys. Rev. Appl.* **13**, 034021 (2020).
- [182] M. Q. Yuan, Y. Zhang, S. H. Yang, C. L. Zhou, and H. L. Yi, Near-field thermal rectification driven by nonreciprocal hyperbolic surface plasmons, *Int. J. Heat Mass Transfer* **185**, 122437 (2022).
- [183] I. Latella and P. Ben-Abdallah, Giant Thermal Magnetoresistance in Plasmonic Structures, *Phys. Rev. Lett.* **118**, 173902 (2017).
- [184] R. M. A. Ekeroth, P. Ben-Abdallah, J. C. Cuevas, and A. Garcia-Martin, Anisotropic thermal magnetoresistance for an active control of radiative heat transfer, *ACS Photonics* **5**, 705 (2018).
- [185] C. Guo, B. Zhao, D. H. Huang, and S. H. Fan, Radiative thermal router based on tunable magnetic Weyl semimetals, *ACS Photonics* **7**, 3257 (2020).
- [186] C. Guo and S. H. Fan, Theoretical constraints on reciprocal and non-reciprocal many-body radiative heat transfer, *Phys. Rev. B* **102**, 085401 (2020).
- [187] L. L. Fan, Y. Guo, G. T. Papadakis, B. Zhao, Z. X. Zhao, S. Buddhiraju, M. Orenstein, and S. H. Fan, Nonreciprocal radiative heat transfer between two planar bodies, *Phys. Rev. B* **101**, 085407 (2020).
- [188] S. Pajovic, Y. Tsurimaki, X. Qian, and S. V. Boriskina, Radiative heat and momentum transfer from materials with broken symmetries: opinion, *Opt. Mater. Express* **11**, 3125 (2021).
- [189] G. Tang, L. Zhang, Y. Zhang, J. Chen, and C. T. Chan, Near-Field Energy Transfer between Graphene and Magneto-Optic Media, *Phys. Rev. Lett.* **127**, 247401 (2021).
- [190] C. Argyropoulos, K. Q. Le, N. Mattiucci, G. D'Aguanno, and A. Alu, Broadband absorbers and selective emitters

- based on plasmonic Brewster metasurfaces, *Phys. Rev. B* **87**, 205112 (2013).
- [191] J. Wu, F. Wu, T. C. Zhao, M. Antezza, and X. H. Wu, Dual-band nonreciprocal thermal radiation by coupling optical Tamm states in magnetophotonic multilayers, *Int. J. Therm. Sci.* **175**, 107457 (2022).
- [192] L. Remer, E. Mohler, W. Grill, and B. Luthi, Nonreciprocity in the optical reflection of magnetoplasmas, *Phys. Rev. B* **30**, 3277 (1984).
- [193] R. Y. Umetsu, K. Kobayashi, A. Fujita, R. Kainuma, and K. Ishida, Magnetic properties and stability of L2(1) and B2 phases in the Co<sub>2</sub>MnAl Heusler alloy, *J. Appl. Phys.* **103**, 07D718 (2008).
- [194] S. Sadat, E. Meyhofer, and P. Reddy, High resolution resistive thermometry for micro/nanoscale measurements, *Rev. Sci. Instrum.* **83**, 084902 (2012).
- [195] D. Thompson, L. Zhu, R. Mittapally, S. Sadat, Z. Xing, P. McArdle, M. M. Qazilbash, P. Reddy, and E. Meyhofer, Hundred-fold enhancement in far-field radiative heat transfer over the blackbody limit, *Nature* **561**, 216 (2018).
- [196] S. Shin, M. Elzouka, R. Prasher, and R. Chen, Far-field coherent thermal emission from polaritonic resonance in individual anisotropic nanoribbons, *Nat. Commun.* **10**, 1377 (2019).
- [197] Y. De Wilde, F. Formanek, R. Carminati, B. Gralak, P. A. Lemoine, K. Joulain, J. P. Mulet, Y. Chen, and J. J. Greffet, Thermal radiation scanning tunnelling microscopy, *Nature* **444**, 740 (2006).
- [198] A. Kittel, W. Muller-Hirsch, J. Parisi, S. A. Biels, D. Reddig, and M. Holthaus, Near-field heat transfer in a scanning thermal microscope, *Phys. Rev. Lett.* **95**, 224301 (2005).
- [199] K. Kim, B. Song, V. Fernandez-Hurtado, W. Lee, W. H. Jeong, L. J. Cui, D. Thompson, J. Feist, M. T. H. Reid, F. J. Garcia-Vidal, *et al.*, Radiative heat transfer in the extreme near field, *Nature* **528**, 387 (2015).